

AMERICAN UNIVERSITY OF BEIRUT

MULTI-FACETED ANTENNA ARRAYS FOR MILLIMETER  
WAVES AND 5G

by  
MARIA NABIL MOUSSA

A thesis  
submitted in partial fulfillment of the requirements  
for the degree of Master of Engineering  
to the Department of Electrical and Computer Engineering  
of the Faculty of Engineering and Architecture  
at the American University of Beirut

Beirut, Lebanon  
May 2018


AMERICAN UNIVERSITY OF BEIRUT

MULTI-FACETED ANTENNA ARRAYS FOR MILLIMETER  
WAVES AND 5G

by  
MARIA NABIL MOUSSA

Approved by:


Dr. Karim Kabalan, Professor  
Electrical and Computer Engineering

  
Advisor

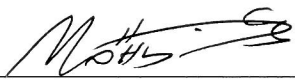
Dr. Hassan Artail, Professor  
Electrical and Computer Engineering

  
Member of Committee


Dr. Youssef Nasser, Senior Lecturer  
Electrical and Computer Engineering

  
Member of Committee

Dr. Mohammed Hussein, Research Associate  
Electrical and Computer Engineering

  
Member of Committee

Dr. Mervat Madi, Research Associate  
Electrical and Computer Engineering

  
Member of Committee

Date of thesis defense: May 2, 2018

# AMERICAN UNIVERSITY OF BEIRUT

## THESIS, DISSERTATION, PROJECT RELEASE FORM

Student Name: Moussa Maria Nabil  
Last First Middle

Master's Thesis                       Master's Project                       Doctoral Dissertation

I authorize the American University of Beirut to: (a) reproduce hard or electronic copies of my thesis, dissertation, or project; (b) include such copies in the archives and digital repositories of the University; and (c) make freely available such copies to third parties for research or educational purposes.

I authorize the American University of Beirut, to: (a) reproduce hard or electronic copies of it; (b) include such copies in the archives and digital repositories of the University; and (c) make freely available such copies to third parties for research or educational purposes after: **One ---- year from the date of submission of my thesis, dissertation, or project.**  
**Two ---- years from the date of submission of my thesis, dissertation, or project.**  
**Three ---- years from the date of submission of my thesis, dissertation, or project.**

Maria

Signature

May 14, 2018

Date

## ACKNOWLEDGMENTS

Foremost, I would like to express my sincere gratitude to my advisor, Professor Karim Kabalan, for the continuous support of my Master's study and research, for his patience, motivation, enthusiasm, and immense knowledge. His guidance helped me in all the time of research and writing of this thesis as well as many other papers that will be published in conferences and journals. He was by my side all the way answering all my questions and giving me helpful instructions. I could not have imagined having a better advisor and mentor for my Master's study.

Besides my advisor, I would like to thank the rest of my thesis committee: Professor Hassan Artail, Dr. Youssef Nasser, Dr. Mohammed Hussein, and Dr. Mervat Madi for their encouragement, insightful comments, and hard questions.

Last, I would like to thank my big family for their endless support throughout the years of my Master's degree especially in under pressure situations.

# AN ABSTRACT OF THE THESIS OF

Maria Nabil Moussa

for

Master of Engineering

Major: Electrical and Computer Engineering

Title: Multi-faceted antenna arrays for millimeter waves and 5G.

Fifth generation networks are the solution of the increasing number of devices and many requirements need to be met when designing such systems. Antennas, used in these systems, are restricted in size and have to have high directive steerable beams and high gain as well as many other requirements. Therefore, the choice of the operating frequency and the used substrate for the antennas create an important challenge in the antenna design process as well as the shape and the size of the antenna to achieve an optimal gain.

In this thesis, planar microstrip antenna arrays having triangular shaped patches as well as multiple three-dimensional antenna designs made of planar antenna arrays of the same size are designed for fifth generation mobile communication systems. All of the proposed antennas are designed on an aluminum oxide ceramic substrate and the 3D antennas are composed of different configurations of planar antenna arrays. The frequency tunability of these antennas is tested on a nine-element antenna array by adding varactors to each patch of it. The capability of beam steering the radiation patterns of these antennas is tested on a MIMO nine-element antenna array by creating different phase shifts on its input points. Also, for the 3D antennas, beam steering was proven to be feasible through a mechanical rotating process of all the planar arrays forming the 3D antenna around one fixed axis.

The simulated results show good matching in all the designs since the reflection coefficients are less -10 dB at around 30 GHz. Gain and radiation patterns of the antennas were also investigated. Obtained simulation results show that these antennas are suitable for millimeter wave communications. The next step will be to fabricate and measure these antennas.

# CONTENTS

ACKNOWLEDGMENTS.....	v
ABSTRACT.....	vi
LIST OF ILLUSTRATIONS.....	ix
LIST OF TABLES.....	xii

Chapter	Page
I. INTRODUCTION .....	1
II. TWO-DIMENSIONAL ANTENNA ARRAY DESIGNS .....	12
A. Single Triangular Patch Antenna .....	12
B. Two-Element Antenna Array .....	15
C. Three-Element Antenna Array .....	18
D. Fractal Design of Nine-Element Triangular Antenna Array .....	21
E. Nine-Element Antenna Array with Triangular-Shaped Ground Plane....	24
III. THREE-DIMENSIONAL ANTENNA ARRAY DESIGNS .....	28
A. Design 1: Three triangular antenna arrays .....	28
B. Design 2: C-Curve .....	29

C. Design 3: 3D Triangle .....	30
D. Design 4: Three-Faces Pyramid .....	31
E. Design 5: Four-Faces Pyramid .....	32
F. Design 6: Right-Standing Three-Faces Pyramid – Crown .....	33
G. Design 7: Cube .....	34
<b>IV. RE-CONFIGURABILITY ASPECTS OF THE ANTENNAS .....</b>	<b>38</b>
A. Frequency tunability using varactors .....	38
B. Beam steering using phase shifts .....	42
C. Beam steering by mechanical rotation .....	48
<b>V. CONCLUSION .....</b>	<b>53</b>
<b>BIBLIOGRAPHY .....</b>	<b>60</b>

## ILLUSTRATIONS

Figure		Page
2.1.	Single patch antenna geometry .....	12
2.2.	$S_{11}$ plot for the single patch antenna .....	14
2.3.	3D Radiation pattern for single patch antenna .....	14
2.4.	Two-element antenna array geometry .....	15
2.5.	$S_{11}$ plot for the two-element antenna array .....	17
2.6.	3D Radiation pattern for the two-element antenna array .....	17
2.7.	Three-element antenna array geometry .....	18
2.8.	$S_{11}$ plot for the three-element antenna array .....	20
2.9.	3D Radiation pattern for the three-element antenna array .....	20
2.10.	Fractal design of nine element antenna array geometry .....	22
2.11.	$S_{11}$ plot for the fractal design of nine-element antenna array .....	23
2.12.	3D Radiation pattern of nine-element antenna array .....	24
2.13.	Nine-element antenna array with triangular-shaped ground plane .....	25
2.14.	$S_{11}$ plot for the nine-element antenna array with triangular-shaped ground plane .....	26
2.15.	3D Radiation pattern for the nine-element antenna array with triangular-shaped ground plane .....	26
3.16.	Three triangular antenna array .....	28
3.17.	Design 1 Gain .....	29
3.18.	C-shaped curve .....	29



3.19.	Design 2 Gain .....	30
3.20.	3D Triangle .....	30
3.21.	Design 3 Gain .....	31
3.22.	Triangular pyramid .....	31
3.23.	Design 4 Gain .....	32
3.24.	Square pyramid .....	32
3.25.	Design 5 Gain .....	33
3.26.	Crown-shaped triangular pyramid .....	33
3.27.	Design 6 Gain .....	34
3.28.	Cube .....	34
3.29.	Design 7 Gain .....	35
3.30.	Effect of spacing between the planar arrays .....	37
4.31.	Nine-element antenna array with varactors .....	39
4.32.	Varactor model used .....	40
4.33.	Reflection Coefficients after the addition of the varactors .....	40
4.34.	Two-dimensional radiation patterns – Varactors .....	41
4.35.	Three-input nine-element antenna array .....	43
4.36.	Reflection coefficients of the three-inputs nine-element antenna array..	44
4.37.	Two-dimensional radiation patterns – Phase shifts .....	45
4.38.	Three-dimensional radiation patterns – Phase shifts .....	46
4.39.	Three inputs MIMO antenna .....	47
4.40.	Two inputs MIMO antenna .....	48

4.41.	Rotational coordinate system of the 3D triangular pyramid .....	49
4.42.	Coordinate systems for the radiation pattern of each triangular plane ...	51
4.43.	Two-dimensional radiation patterns – Mechanical rotation .....	51
4.44.	Three-dimensional radiation patterns – Mechanical rotation .....	52

## TABLES

Table		Page
2.1.	Single patch antenna dimensions .....	13
2.2.	Two element antenna array dimensions .....	16
2.3.	Three-element antenna array dimensions .....	19
2.4.	Nine-element antenna array dimensions .....	22
2.5.	Nine-element antenna array with triangular-shaped ground plane dimensions .....	25
4.6.	Three phases combinations .....	44

# CHAPTER I

## INTRODUCTION

FIFTH generation networks [1] present the future most demanded technology in the next major phase of mobile telecommunications as it addresses many advanced features overpassing the preceding technologies. Some of these features are good throughput, high bit rate, larger coverage range, better energy consumption as well as multiple concurrent path, which makes it able to serve billions of connected devices. As more users come online, the authors of [2] stated that 4G networks have reached the limit at a time when users want even more data for their devices. The highly efficient systems, the uniform service experience in a cell, and the use of higher frequency bands are the most important challenges when implementing 5G wireless systems as stated by [3]. Comparing to 4G bands, bandwidth coverage of the 5G is enhanced by ten times using a new transmission band that makes it possible for higher data rates. According to [4], the specific frequency bands from 3 GHz to 30 GHz are known as super high frequency band and the frequency range from 30 GHz to 300 GHz are known as extremely high frequency bands. The 3-300 GHz is also named millimeter wave frequency band with wavelengths from 1 to 100 millimeters, since the two previous frequency bands has similar propagation characteristics.

The realization of millimeter wave wireless communications necessitate the design of millimeter wave antennas as a first step as indicated in [4]. These antennas are required to have highly directional patterns, for the purpose of long transmission range as well as high detection sensitivity, and to have a reduced size with a sufficient impedance

bandwidth. Compact and efficient antennas are required for an efficient deployment of the 5G systems [5]. Moreover, to fit into handheld devices, these antennas have to be small in size. Other requirements of these antennas used in 5G technology, as outlined in [6], is having a radiation pattern with beamforming capability to be able to perform spatial scanning.

When designing antennas at millimeter waves, there will be a trade-off between many characteristics such as: technological design issues, low cost, which is a commercial issue, small size, radiation efficiency, gain, broadband performance, and many more. For the performance of these antennas, a reflection coefficient less than or equal to -6dB is acceptable for operation in the mobile antenna standards, [7].

Higher frequency bands used in 5G systems suffer from high propagation loss, which brings us to the concept of small cells that overpass the existing 4G macro cells. To reduce high path loss at this band, the access point need to be brought closer to the user in order to reduce the signal path and that is achieved by having very limited cell radius. Other limiting factors of using millimeter waves for cellular purpose are foliage losses, rain attenuation, and high penetration. Wavelengths at these frequencies have approximately the same size as the rain drop and that's what cause high signal scattering. The attenuation gets worst when the frequency is higher, therefore the lower boundary of the millimeter waves frequency band having the longer wavelength presents the lowest attenuation and that brings us to the choice of operation at 30 GHz. Therefore, when designing antennas for millimeter wave 5G, one should take into account the atmospheric absorption at millimeter waves, which leads to high propagation losses.

Since we already mentioned that these antennas have to be small in size, the type of the antenna that suits this requirement is microstrip antennas. A microstrip patch antenna, as indicated in [8], is decomposed of a dielectric substrate that has a radiating patch, which is usually made of copper on one side and a ground plane on the other side. The radiation exists primarily because of the fringing fields between the edge of the patch and the ground plane. When comparing microstrip patch antennas to conventional microwave antennas, [9], it is noticed that microstrip patch antennas are small in size, have a light weight, low cost, simple to manufacture and easy to integrate in mobile radio and other wireless communication devices. Concerning the shape of the patch, the triangular shaped patch antenna is among the shapes that attracted much attention, [10]. The main reason of this attraction is their small size when compared to other shapes such as the rectangular and the circular patch antennas. After choosing the type of the antenna and the shape of the patch, a careful analysis should be done now on the dimensions of the patch, [11]. The results such as the resonant frequency, the bandwidth, the directivity and the gain could be changed significantly if a small change of any dimension occurs.

Another important step in designing a microstrip patch antenna is the choice of the substrate that suits the application targeted by this antenna. The dielectric constant of the substrate used and the size of the antenna are inversely proportional, [12], i.e. the higher the dielectric constant the smaller the size of the antenna, however there is a trade-off with the operating bandwidth, which will become narrower. Because of the low dielectric constant of the traditional substrates, they could not be used to fabricate small size antennas, [13]. A better choice will be the ceramics with higher dielectric constant that will help reducing the

size of the antenna. Obviously the patch size and the length of the transmission line have a direct effect on the return loss and the resonant frequency of the designed patch antenna. Additionally, the quality factor of ceramic is large in the microwave range and since the quality factor is inversely related to the return loss, the return loss will be reduced when using the ceramic boards. The choice of the aluminum oxide ceramic substrate is based on the fact that it has a high dielectric constant as well as a zero tangent loss, [14]. An antenna designed using this substrate will have a reduced size and a much better performance in terms of bandwidth, gain, and efficiency when compared to other substrates such as Rogers and FR4 epoxy.

Using a thick substrate will result in an increase in the overall gain as well as the bandwidth of the antenna, [15], because the radiation power will increase and the conductor loss will be reduced. This leads to an antenna that is heavy and bulky and the dielectric losses and the surface wave losses will increase, so there will be a tradeoff between the thickness of the substrate, the antenna size, and its performance. Therefore, when the designer is not restricted by a small size of the patch, it is preferred to use substrates with low dielectric constants. In our case, after a good study on the substrates, an aluminum oxide ceramic substrate with a dielectric constant of 9.8 and a thickness of 0.254 mm turned out to be a good choice.

When the basic goal of a design is to achieve a certain performance at a specific operating frequency, an antenna element can be used alone or combined with other elements to form an array, [10]. Additionally, to compensate for high path loss at millimeter frequency bands, millimeter waves tend to use highly directional antennas.

Another goal to be achieved is high gains and low side lobe levels in some desired directions, so the best solution are planar arrays that allow obtaining directive beams, [16]. The selection of the number of elements in the antenna array as well as its structure leaves a very wide open door for a big range of optimization problems. To compensate for the high free space losses that could be encountered, short range communications are needed, which require high gain antenna arrays. So the design has to be efficient and compact in size to fit on the edge of a handheld device. To enhance the gain or provide beam scanning capability, [11], many practical systems use antenna arrays. When designing antenna arrays, an important issue to take into account is the mutual coupling between the antenna elements, which could modify the radiation pattern, the beam width, and the directivity of the array. A maximum gain of an array could be obtained when an optimization is done on the mutual coupling and the passive reflection coefficient, that is because the mutual coupling is a natural effect that could be desirable sometimes in the behavior of the array. So a non-zero value of mutual coupling could be sometimes beneficial.

A third dimension is usually added to the array if the antenna is supposed to provide additional gain, [17], with limitation in the area. This could be solved by placing multiple arrays in a certain configuration. Placing multiple antenna arrays inside the mobile handset allows the flexibility of operating in multiple configurations by the fact of being able to excite one array at a time or multiple arrays at the same time, [5]. To explain more the advantages of these configurations, the authors of [16] considered the example of three planar arrays placed in a triangular configuration, each array can cover a sectored cell in its own direction. Also, when having high gain antennas, the communication between each



user with the base station will be approximately interference-free because directive beams will be higher and side lobe levels will be lower. In our case, to get a good suppression of side lobe levels, [10], the triangular patch antenna array is a better choice than the rectangular patch antenna array.

Many similar antennas could be found in the literature. A very simple patch antenna is proposed in [9]; it operates at 38.14 GHz with a return loss of -31dB. It has a compact size, which makes it suitable for the next generation 5G wireless communication devices. It is fed using a coaxial probe feed and the substrate used is a Taconic RF-60™ substrate with a dielectric constant of 6.15. However more sophisticated patch antennas could be designed to meet up with the requirements of the future 5G networks. In [18], a slotted patch antenna operational at two frequency bands 28 GHz and 38 GHz is proposed. It is used in highly demanded MIMO systems in 5G networks. Some measurement results are presented, which proves its performance in the near-field as well as the far-field. Two elements and four elements linear triangular patch antenna arrays are presented in [10] and a comparison was made between rectangular and triangular antenna arrays of the same size. The feeding network of the two elements is formed of 50 ohms input impedance split into two 100 Ohms transmission lines. However, a quarter wave transformer is used to feed the four elements array. It is proven that a triangular antenna array has approximately the same performance of a rectangular antenna array but a better suppression of side lobe level could be achieved using the triangular shape. Also in [19], an array of four triangular patches is designed. It operates at 5.5 GHz and it is designed on an FR4 substrate with a dielectric constant of 4.4. The feeding network is also designed using a quarter wave transformer.

Simulated results agreed with the measurements with an  $S_{11}$  of approximately -32dB and a VSWR less than 2 as well as a high directivity. The authors of [20] designed a phased array antenna that consists of eight 28 GHz Vivaldi antenna. The simulations showed a reflection coefficient less than -10dB, a good gain, high efficiency and 3D beam steering characteristics in the band of operation and that makes it a good candidate for millimeter wave 5G communications. The authors of [21] proposed a compact 3D antenna for LTE, GSM and UMTS vehicular applications. Two identical antennas of this type are considered together to form a MIMO system. Thanks to the small size of the single radiating element, it can be considered as a good candidate to be integrated under the shark-fin cover of a vehicle. Four types of 3D antenna structures are presented in [22] and each type showed an improvement in the performance of the antenna. Two of the four types designed, presented maximum current at their surface, which allowed the insertion of the feed deeper in the antenna and therefore making the size of the antenna more compact. Also the sizes of the 3D antennas designed, exhibited reduction compared to the planar antennas designed for the same application. The improved antenna parameters such as its compact size as well as the wider bandwidth offers many benefits to on chip applications.

Great attention is being focused on re-configurable antennas especially in the future wireless communication systems thanks to their ability to reduce front-end system and to allow pre-filtering at the receiver. A re-configurable antenna is an antenna that is capable of re-configuring its characteristics such as frequency, radiation pattern, bandwidth and polarization to adapt to the environment, [23]. Besides their re-configurable capability,

re-configurable antennas contain many other features such as low cost, size miniaturization and multipurpose functions and they use micro-strip antennas as a platform.

In addition, recent systems must be able to receive signals over a wide range of frequencies so they require, as stated in [24], either wide-band or tunable antennas. The requirement of receiver filters is relaxed because tunable narrow-band antennas, in contrary to broadband antennas, provide frequency selectivity. Tunable antennas, [25], are of interest for wireless communication systems because they could substitute multiple antennas operating at different frequencies, which will reduce the implementation size and its cost as well as the complexity of the system. Another advantage presented by such antennas is the ability to reject the interference from services coexisting in the spectrum. Slot antennas are one of the common types of antennas used in frequency tuning because varactors or switches could be used easily to change their resonant frequency. [26], [27] and [28] are some of the examples of such antennas found in the literature. The frequency tuning is achieved by varying the effective length of the slots using varactor diodes embedded across the slots.

A tunable antenna could be obtained by loading the patch antennas with varactor diodes, [29], thus having a change in the resonant frequency of the patch. In the literature review, we could find some designs that implement varactors between the patch and the ground plane, however, in this thesis, the varactors are placed on the transmission line branches that form the feeding network, and each varactor is placed before the transmission line arrives to the inset feeding position of the triangular patch.

A small research could be done on some of the interesting tunable antenna designs. The authors of [26] present a slot antenna that uses switches to change its electrical length and having an effective wide bandwidth. A small patch antenna that could be tuned between 800 MHz and 900 MHz is designed in [30], this antenna uses variable capacitors and transistors. The controlling was done using a radio baseband processor that sends commands to a digital control unit implemented in the antenna. In [27], a slot antenna is loaded with two lumped variable capacitors, also known as varactors, placed in properly chosen positions along the slot. The antenna obtained is a dual-band antenna having two operational frequencies that could be controlled individually. In [31], RF-MEMS switches are integrated with self-similar planar antennas, which showed re-configurable properties; radiation patterns are kept similar over a wide frequency range. In [32], a reconfigurable triangular microstrip patch antenna is realized using RF-MEMS switches also to demonstrate a monolithic passive electronically scanned array having a low cost.

The effect of implementing varactors in the nine-element antenna array of this thesis, is investigated in terms of frequency tunability. After placing the varactors in their most suitable positions, the capacitance is then varied so that the resonant frequency of the antenna is shifted. The electronic tuning will be realized by changing the applied DC voltage, when the varactors are used with their appropriate biasing network, [26]. In addition, the antenna's efficiency and the realized gain could be affected by the integration of the varactors.

In this thesis, a triangular microstrip patch antenna is simulated using an aluminum oxide ceramic substrate with a dielectric constant of 9.8 and a thickness of 0.254 mm. It is

operational at 30 GHz with a reflection coefficient of -42dB and a gain of 5.9dB. In a way to increase the directivity and the gain of the antennas, the number of elements is increased as well as the gains having 8.57 dB, 9.26 dB, 12.51 dB and 13.13 dB for the two-elements, three-elements, fractal design of three-elements forming nine elements and the same fractal design with a triangular shaped ground plane, respectively. All of the designs are matched at around 30 GHz. A parametric study was done on the side length of the triangle, the width of the transmission lines forming the feeding network, the length and width of the gap and the length of the 50 Ohms transmission line feeder to get the best gain in each design with the lowest  $S_{11}$  possible at 30 GHz.

A third dimension is added to the arrays designs because additional gain is required but the area inside a handheld device is limited. Multiple configurations could be done by placing several planar antenna arrays in proximity to each other with a convenient spacing between the arrays, chosen after a parametric study to achieve the best gain possible with a trade-off between the gain and the size of the antenna.

Varactors were added to the nine-element antenna array to check its frequency tunability. Frequency was tuned to multiple different frequencies falling between 20 GHz and 35 GHz and having similar radiation patterns.

Finally, beam steering capability was tested using two approaches: applying a rotational movement to the 3D triangular pyramid design around a fixed axis, and exciting the inputs of a MIMO antenna array with different phase excitations.

This thesis is divided into five chapters. Chapter II presents the simulated designs of all the planar microstrip two-dimensional patch antenna arrays. The three-dimensional designs are presented in chapter III. Chapter IV investigates the results of some re-

configurable antennas in terms of frequency tunability and beam steering capability. Finally, the thesis will be concluded in chapter V.

## CHAPTER II

### TWO-DIMENSIONAL ANTENNA ARRAY DESIGNS

#### A. Single Triangular Patch Antenna

First, a triangular shaped patch antenna, shown in Fig. 2.1, is designed to operate at 30 GHz. Eq. (1) is used to determine the side length of the equilateral triangle, [10], where  $c$  represents the velocity of electromagnetic waves in free space,  $\epsilon_r$  is the dielectric constant of the substrate,  $a$  is the side length, and  $f$  is the resonant frequency. This equation relates the side length of the patch with its resonance frequency.

$$f = \frac{2c}{3a\sqrt{\epsilon_r}} \quad (1)$$

After using the parameters chosen as discussed in the introduction, the value of  $a$  is found to be 2.13 mm; however, this value is only considered as a start point. A parametric study has to be done on this dimension to find the best value for a good performance at 30 GHz.

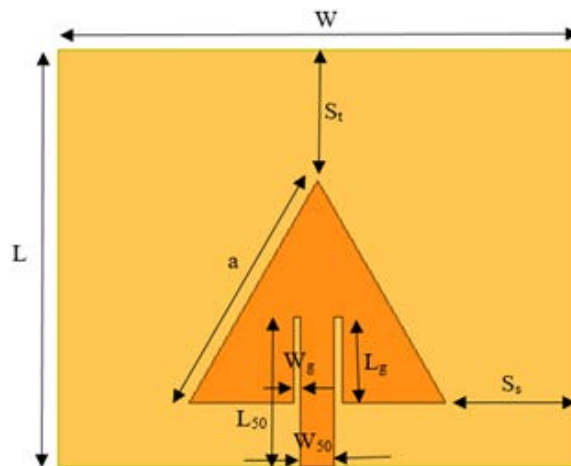


Figure 2.1. Single patch antenna geometry

A parametric study was done on other parameters such as the side length of the triangular patch, the spacing between the patch, the edges of the substrate from the top and at both sides, the width and length of the inset feed as well as the width and the length of the gap where the feeding point is chosen. The values chosen for these parameters are presented in Table 2.1.

TABLE 2.1. Single patch antenna dimensions

<i>Parameter</i>	<i>Value</i>
$L$	3.187 mm
$W$	3.96 mm
$a$	1.96 mm
$S_t$	1 mm
$S_s$	1 mm
$W_g$	0.06 mm
$L_g$	0.66 mm

The 50  $\Omega$  transmission feed line has a fixed width,  $W_{50}$ , of 0.25 mm at 30 GHz using the substrate with 9.8 dielectric constant and a length,  $L_{50}$ , of 1.15 mm. The length and width of the transmission lines are found using LineCalc from ADS. Matching is very good at 30 GHz since the reflection coefficient is far below -10 dB, as shown in the  $S_{11}$  plot of Fig. 2.2. Also, this single triangular patch antenna has a gain of 5.97 dB as shown in Fig. 2.3, which shows also the three-dimensional radiation pattern of the single triangular patch antenna.



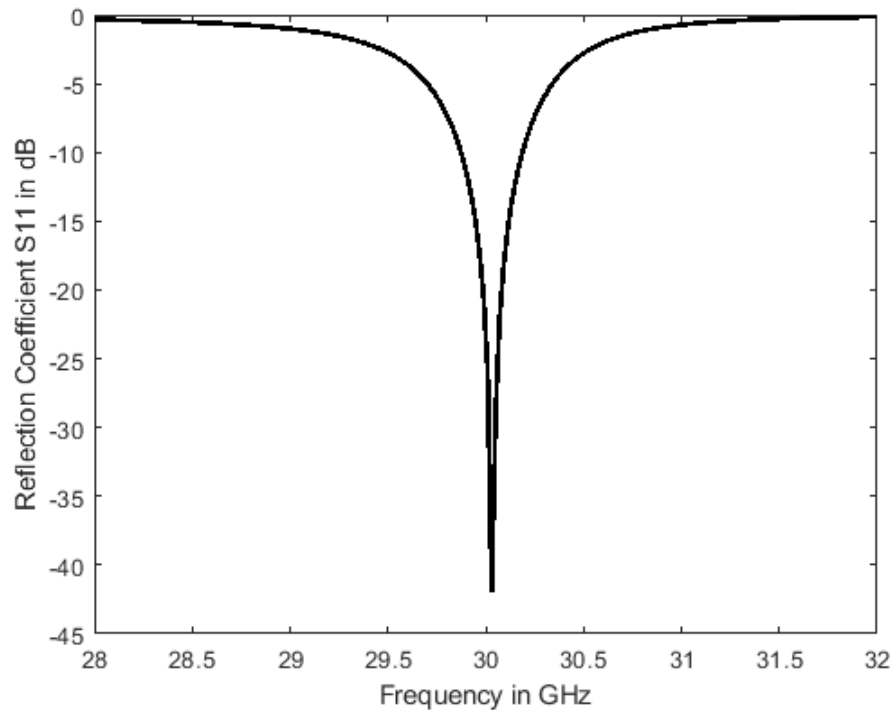


Figure 2.2. S<sub>11</sub> plot for the single patch antenna

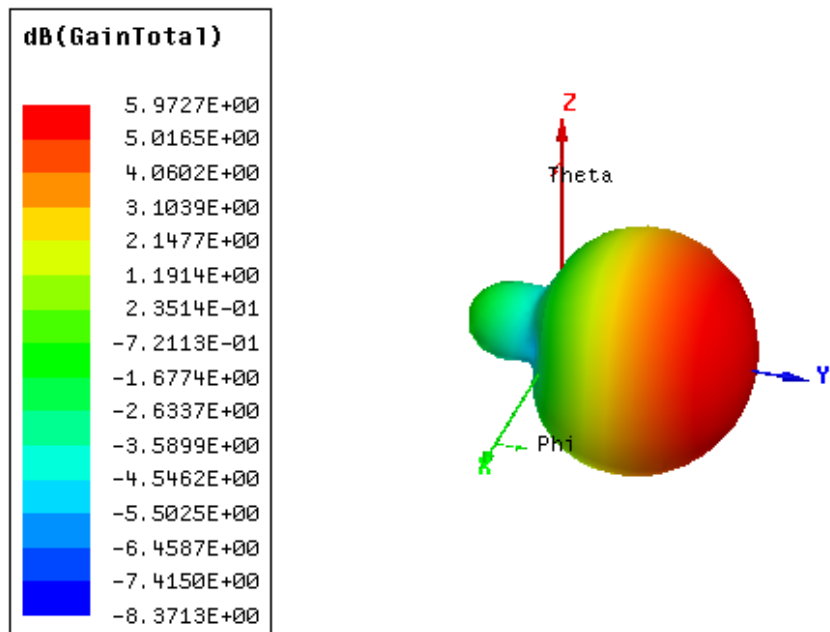


Figure 2.3. 3D Radiation pattern for single patch antenna

This antenna has a good performance in terms of gain, however it is supposed to have additional gain and higher directivity, so a second element was added.

### B. Two-Element Antenna Array

Fig. 2.4 shows the configuration of a two-element triangular patch antenna array. The impedance of the input transmission line feeder is  $50 \Omega$  with the same length and width of 1.15 mm and 0.25 mm respectively; this line is split into two  $75 \Omega$  lines with widths,  $W_{75}$ , 0.09 mm at the chosen frequency of operation and using this specific substrate. The performance is found to be at its best when the spacing between the two elements is a half wavelength. After a parametric study on the different parameters of this array, the values chosen are presented in Table 2.2.

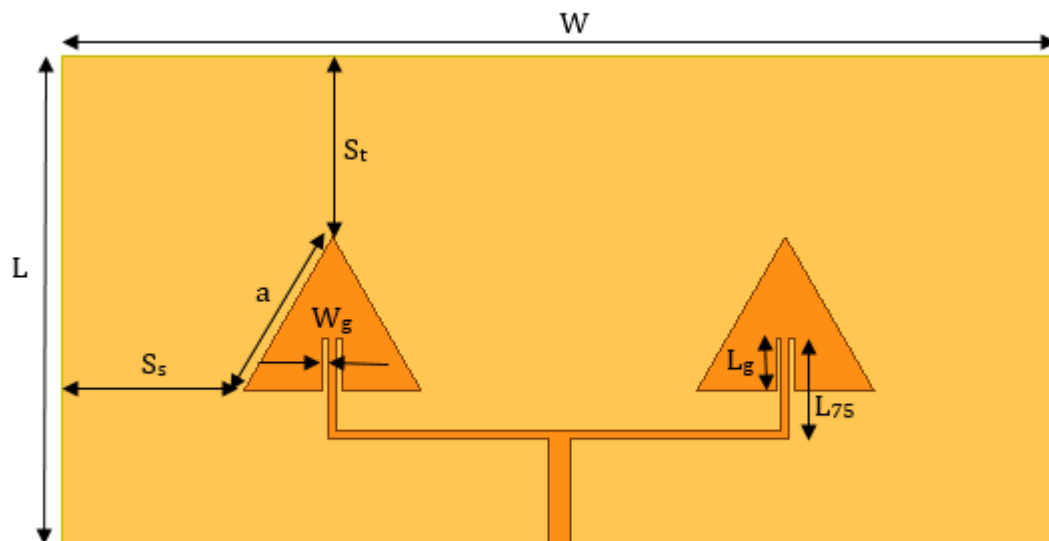


Figure 2.4. Two element antenna array geometry

TABLE 2.2. Two element antenna array dimensions

<i>Parameter</i>	<i>Value</i>
$L$	5.376 mm
$W$	10.959 mm
$a$	1.959 mm
$S_t$	2 mm
$S_s$	2 mm
$W_g$	0.06 mm
$L_g$	0.58 mm
$L_{75}$	1.02 mm

It is worth to mention that the side length of the triangular patch is slightly different from the single element antenna and that in order to have perfect matching at 30 GHz. Obviously, as shown in Fig. 2.5, this design resonates at approximately 30 GHz with a different value of reflection coefficient than the one obtained for the single element. Fig. 2.6 shows the three dimensional radiation pattern of the two-element antenna array. Note that the gain obtained is 8.44dB, hence the gain increased by 45% by creating a two element array.

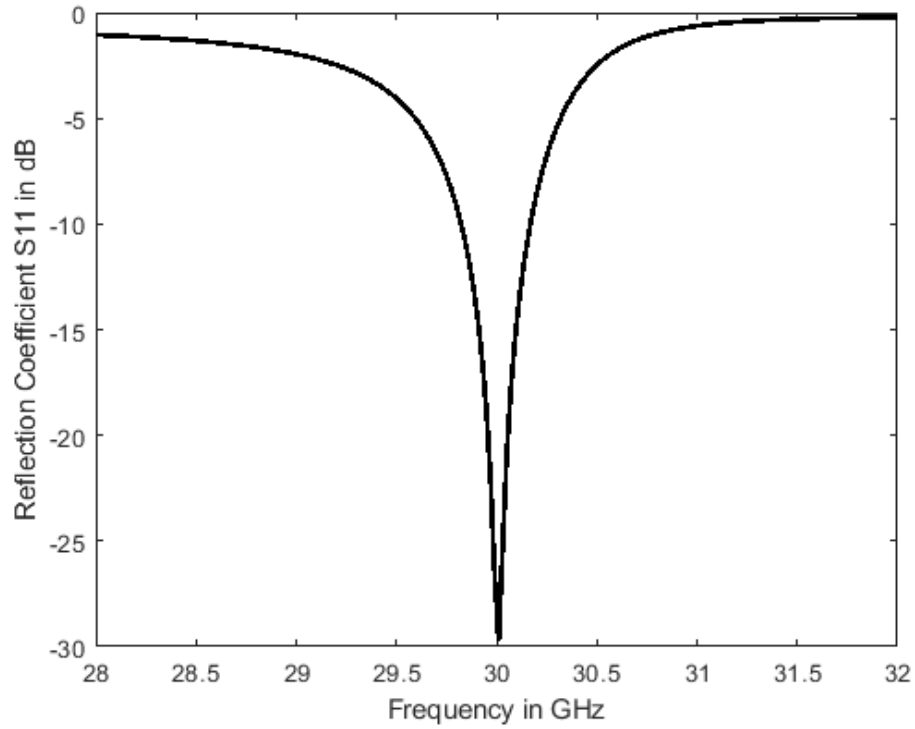


Figure 2.5.  $S_{11}$  plot for the two-element antenna array

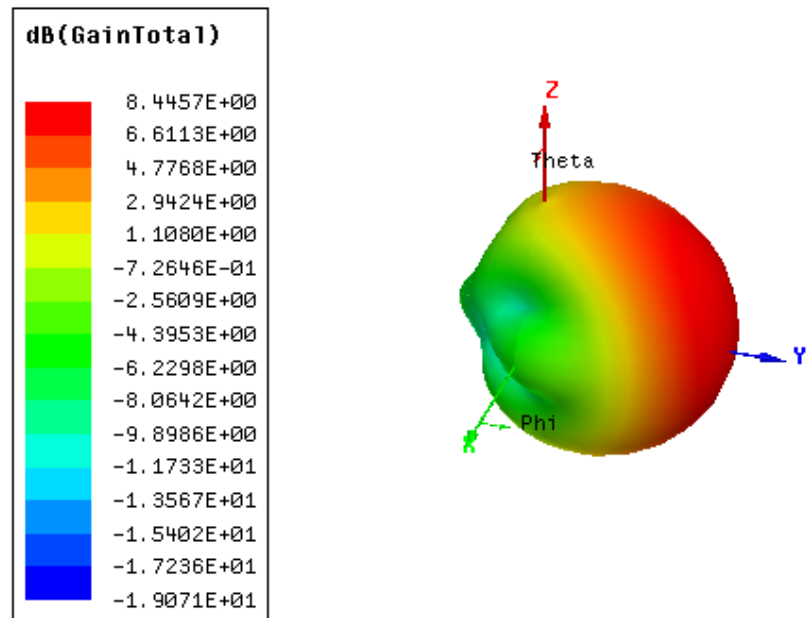


Figure 2.6. 3D Radiation pattern of the two-element antenna array

As already stated, the gain has improved but the increase achieved is not enough so a third element had to be added to further improve the gain and increase the directivity of the antenna.

### C. Three-Element Antenna Array

In order to further enhance the gain of the antenna, a third triangular patch is added to the array. Fig. 2.7 shows the three-element antenna array and its dimensions are given in Table 2.3. The spacing between the elements placed horizontally is equal to half-wavelength however the third element is placed above the two by a distance of a quarter wavelength.

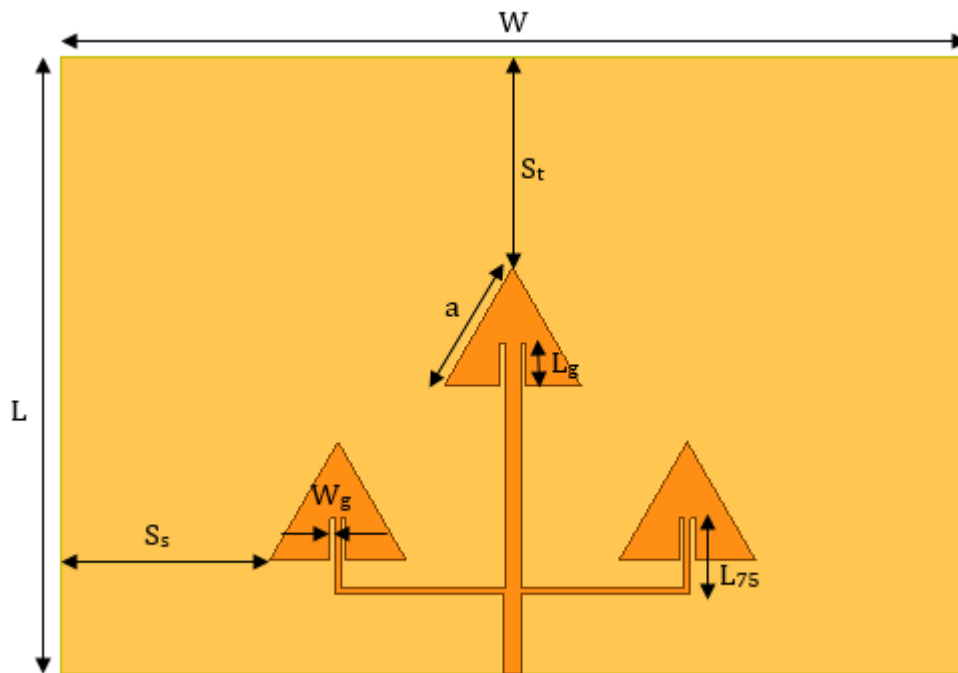


Figure 2.7. Three-element antenna array geometry

TABLE 2.3. Three element antenna array dimensions

<i>Parameter</i>	<i>Value</i>
$L$	8.828 mm
$W$	12.95 mm
$a$	1.95 mm
$S_t$	3 mm
$S_s$	3 mm
$W_g$	0.07 mm
$L_g$	0.6 mm
$L_{75}$	1 mm

The  $50 \Omega$  transmission feed line is split into three lines: two  $75 \Omega$  transmission lines that feed the two horizontally placed triangular elements and a third transmission line that has a value of approximately  $50 \Omega$  to feed the upper triangular patch. This configuration turned out to have the best gain of 8.71dB as shown in Fig. 2.9 representing the three dimensional plot of the radiation pattern for the array of three elements. A good matching at a frequency around 30 GHz is achieved as shown in Fig. 2.8. Fig. 2.9 shows that the three-element antenna array has a higher directivity than the previous two antenna arrays, which validates the use of larger antenna arrays for directive millimeter wave propagation.

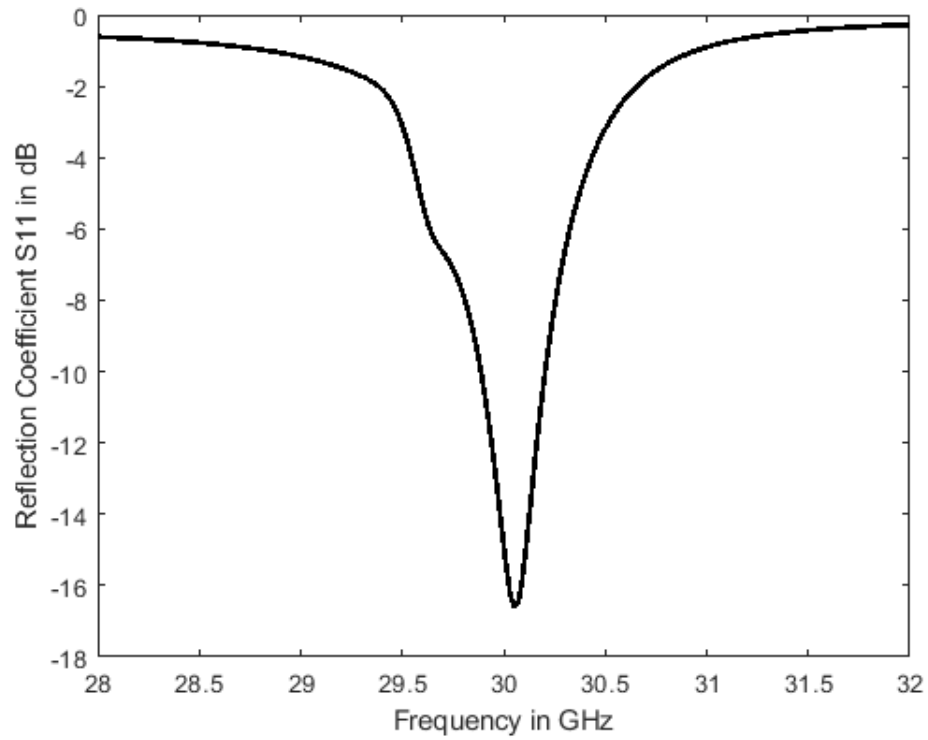


Figure 2.8.  $S_{11}$  plot for the three-element antenna array

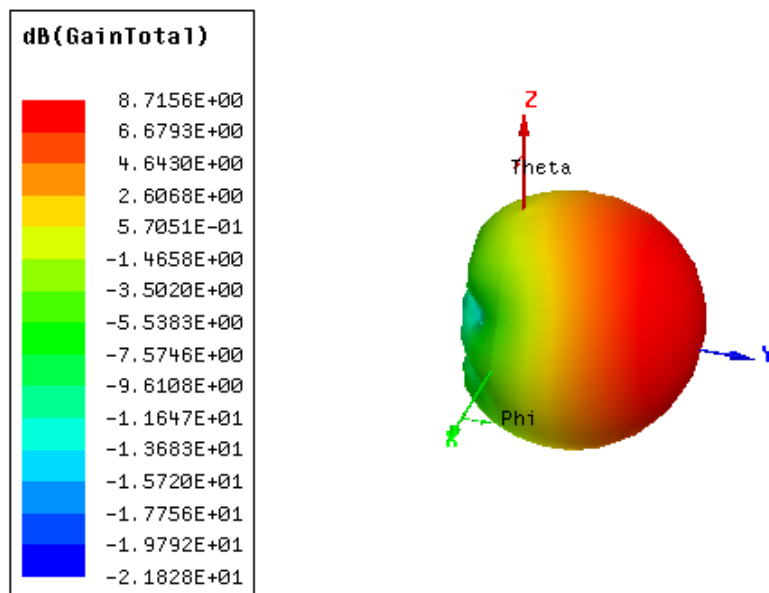


Figure 2.9. 3D Radiation pattern for the three-element antenna array

The gain slightly increased by about 0.3dB seeing the feeding network for three elements was not previously designed and a parametric study had to be done on the widths of the transmission lines to find the best performance. Since additional gain is an attractive characteristic for such antennas, fractal design could be introduced to improve the gain without highly enlarging the size of the antenna.

#### **D. Fractal Design of Nine-Element Triangular Antenna Array**

B. Mandelbrot proposed, in [33], the fractal theory, which states that, in contrast with the Euclidean space, the space can have a fractional dimension based on the repetition of a certain shape. [34] proposed that a fractal geometry has a space-filling property, which will result in designing miniature classic antenna elements. As explained in [35], a repeated application of the generator produces this self-similar structure, and in the case of the fractal design of this antenna, the generator is defined as the three-element triangular patch antenna. This design has three branches by repeating the generator three times. The two branches at the bottom are the parents and the one at the top is the child branch.

In this thesis, the fractal design is generated by repeating the three-element triangular antenna array, three times; the three three-element antenna arrays are placed in a triangular shape also. Fig. 2.10 presents the geometry of the biggest antenna array of nine elements, designed using the previous three-element antenna array by the fractal design procedure. The dimensions of this antenna are presented in Table 2.4.



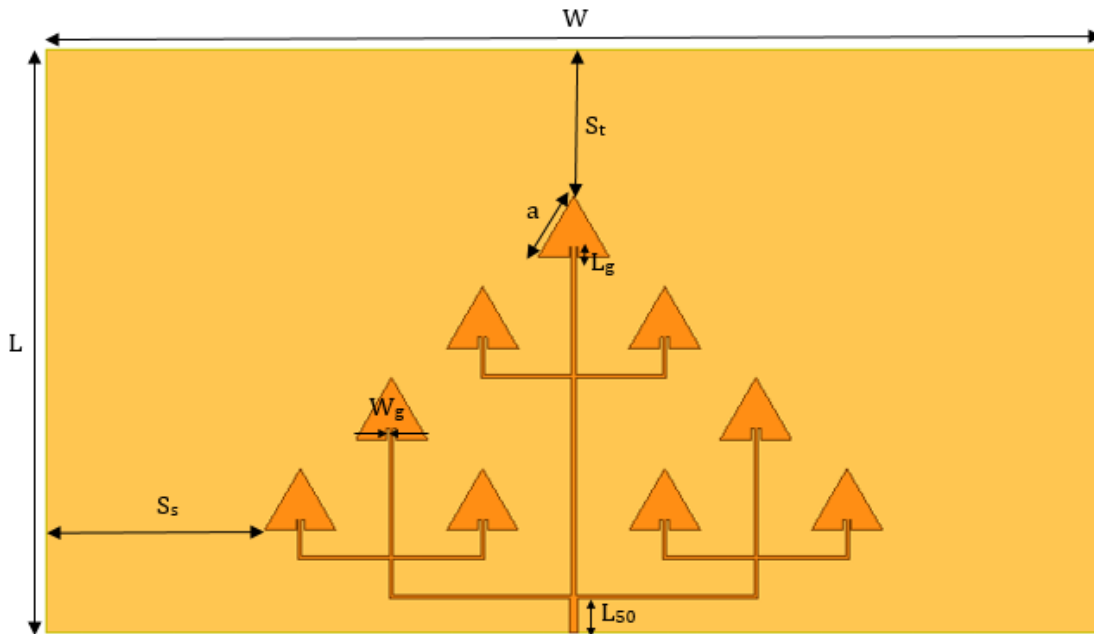


Figure 2.10. Fractal Design of nine-element triangular antenna array geometry

TABLE 2.4. Nine-element antenna array dimensions

<i>Parameter</i>	<i>Value</i>
$L$	16 mm
$W$	28.96 mm
$a$	1.96 mm
$S_t$	4 mm
$S_s$	6 mm
$W_g$	0.08 mm
$L_g$	0.3 mm
$L_{50}$	0.92 mm

In this design, the feeding network is formed of the  $50 \Omega$  transmission line feeder split equally into three  $75 \Omega$  transmission lines, which are, in turn, split into three  $75 \Omega$  transmission lines also. The side length of the triangular patches regained its size of 1.96 mm. A parametric study was done on several design parameters such as the side length of the triangle, the length and width of the inset feed, the spacing between the radiating patch,

the edges of the substrate, and the length and width of the transmission lines. Also, a parametric study was done on the spacing between the three-element triangular antenna arrays. Each array presents an element of the fractal design; the spacing between the horizontally placed elements is a full wavelength, which makes it a half-wavelength between each single triangular patch. The spacing between the two lower arrays and the one placed above them is also a half-wavelength. Fig. 2.11, the  $S_{11}$  plot, shows a good matching condition at 30 GHz and Fig. 2.12, the 3D plot of the radiation pattern, represents a gain of 12.11dB and the radiation pattern is becoming more and more directive.

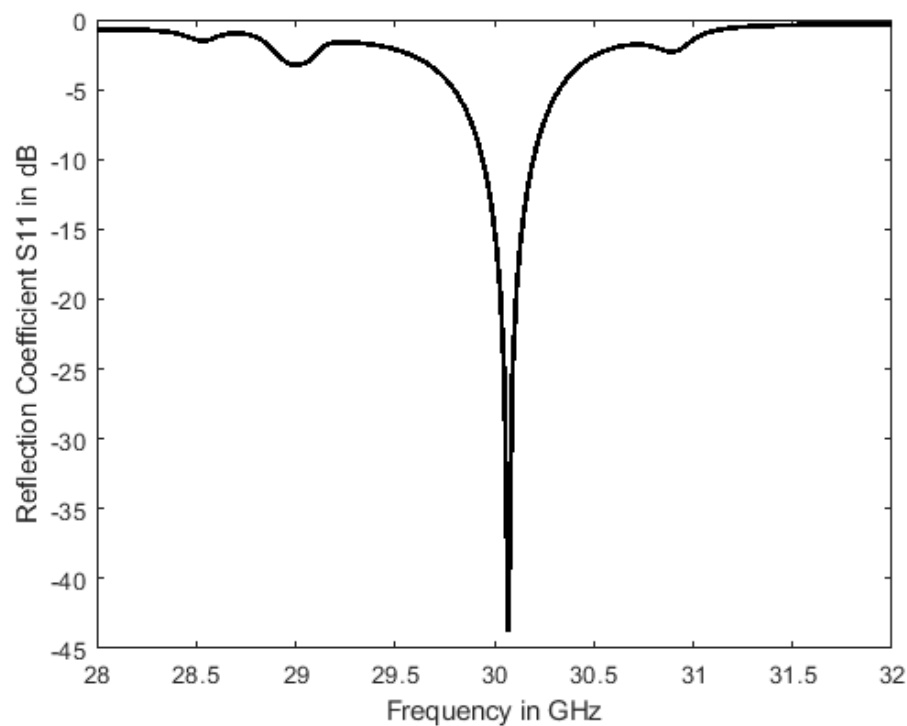


Figure 2.11.  $S_{11}$  plot for the fractal design of nine-element triangular antenna array

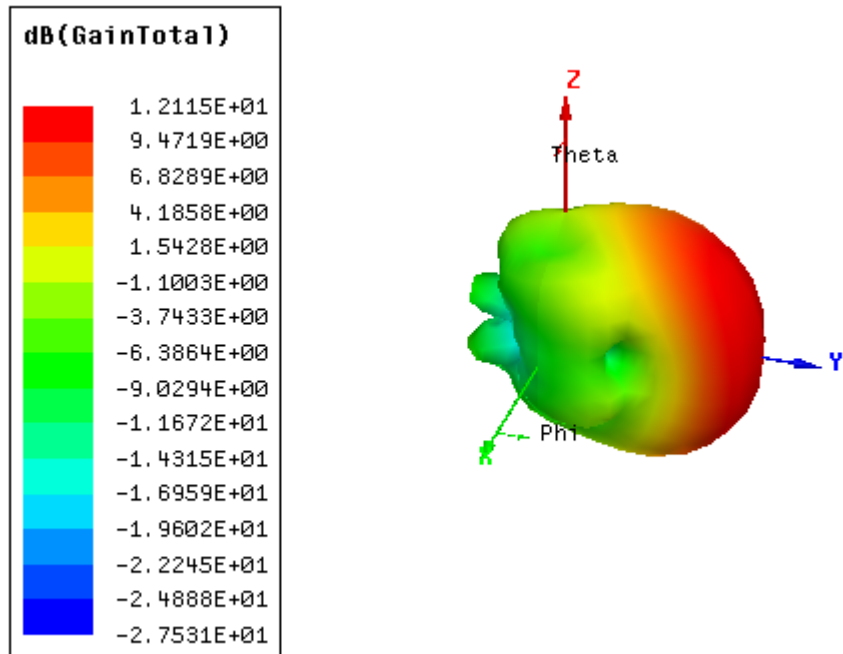


Figure 2.12. 3D Radiation pattern of nine-element triangular antenna array

A novel idea was to try the triangular-shaped substrate and check its performance in terms of gain and efficiency.

### E. Nine-Element Triangular Antenna Array with Triangular-Shaped Ground Plane

In the same previous design of nine elements, the ground plane is cut into a triangular shape and the new antenna array is shown in Fig. 2.13 with all its dimensions in Table 2.5. Its reflection coefficient plot, shown in Fig. 2.14, presents good matching conditions at 30 GHz and its gain slightly increased to 12.41dB as depicted in Fig. 2.15. Some parameters, such as the side length of the triangular patch and the width and length of the inset feed, have changed just to maintain a good performance at 30 GHz with a high

gain; however, the spacing between all the elements, the spacing from the edges and the feeding network design are kept unchanged.

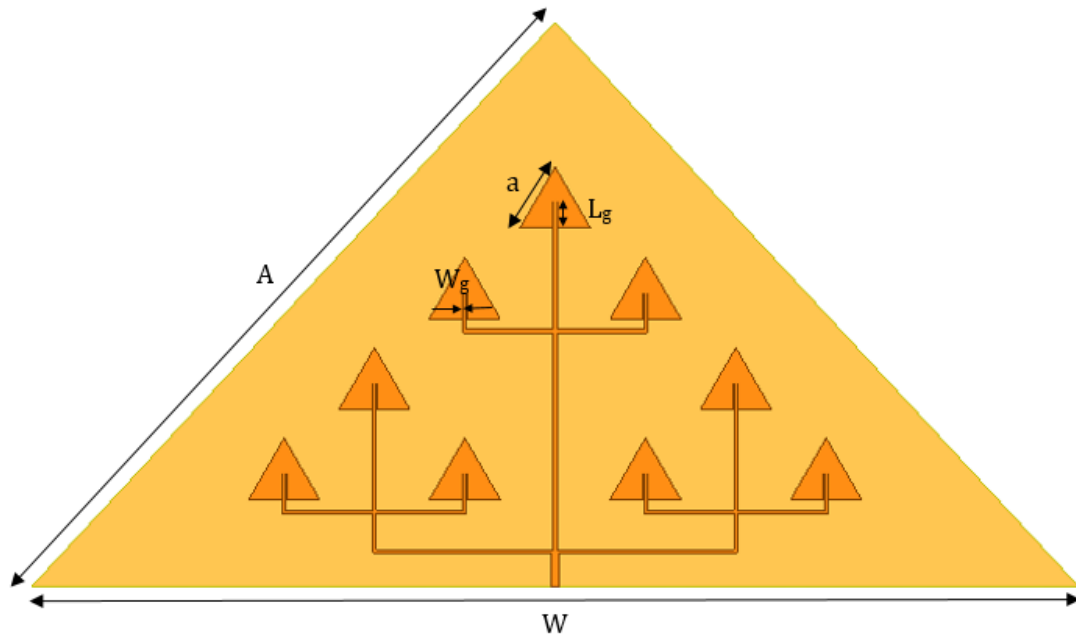


Figure 2.13. Nine-element antenna array with triangular-shaped ground plane

TABLE 2.5. Nine-element antenna array with triangular-shaped ground plane dimensions

<i>Parameter</i>	<i>Value</i>
$A$	21.57 mm
$W$	28.96 mm
$a$	1.959 mm
$W_g$	0.02 mm
$L_g$	0.3 mm

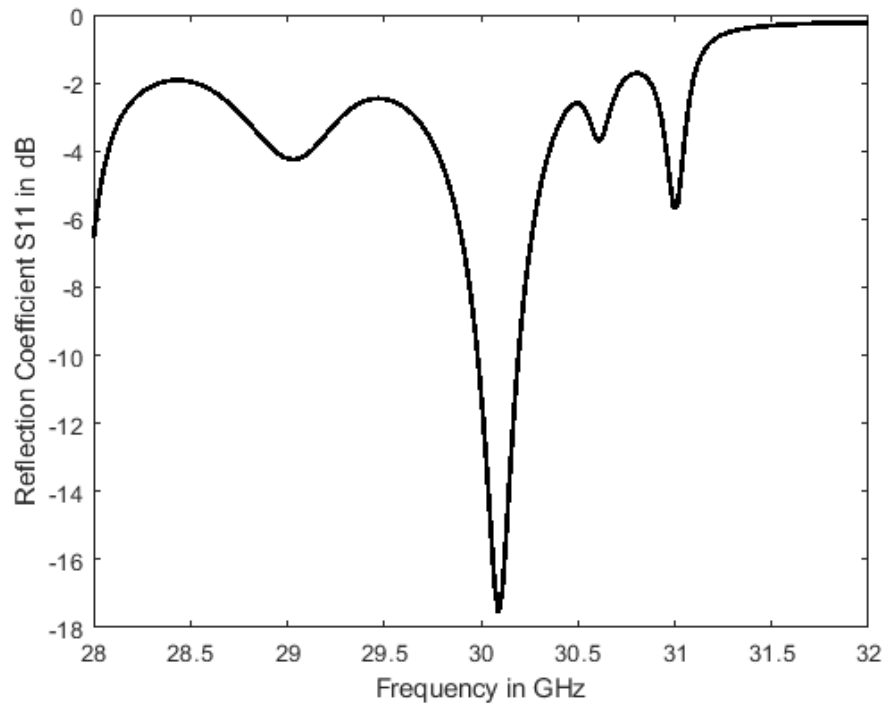


Figure 2.14.  $S_{11}$  plot for the nine-element antenna array with triangular-shaped ground plane

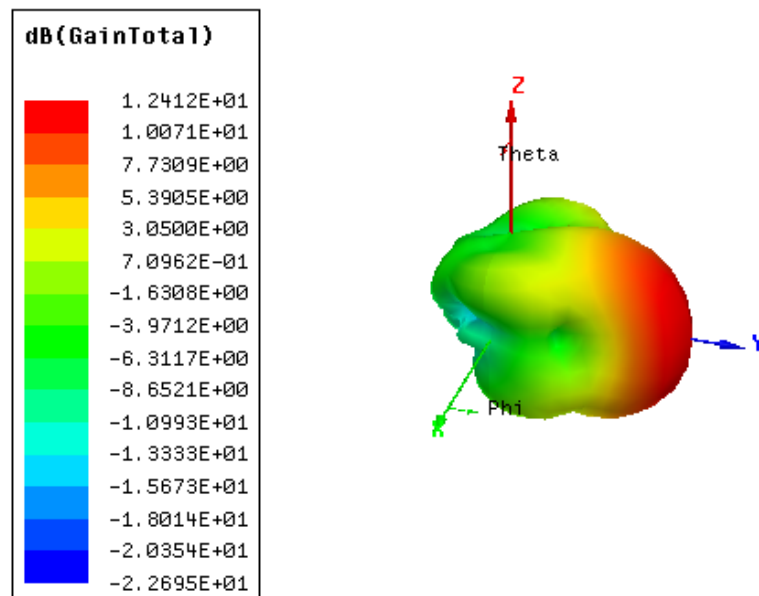


Figure 2.15. 3D Radiation pattern of nine-element antenna array with triangular-shaped ground plane

Since the last two designs presented the best gain so far, they will be used to produce three-dimensional designs in the next chapter.

## CHAPTER III

### THREE-DIMENSIONAL ANTENNA ARRAY DESIGNS

In all the following three-dimensional designs, all the planar antenna arrays exhibit a small shift in their resonant frequency; however, a very well matching condition at 30 GHz is achieved in all cases. The following three-dimensional designs are obtained by placing multiple two-dimensional antenna arrays in different configurations. These 3D designs are cited in descending order, from highest to lowest gain.

#### A. Design 1: Three triangular antenna arrays

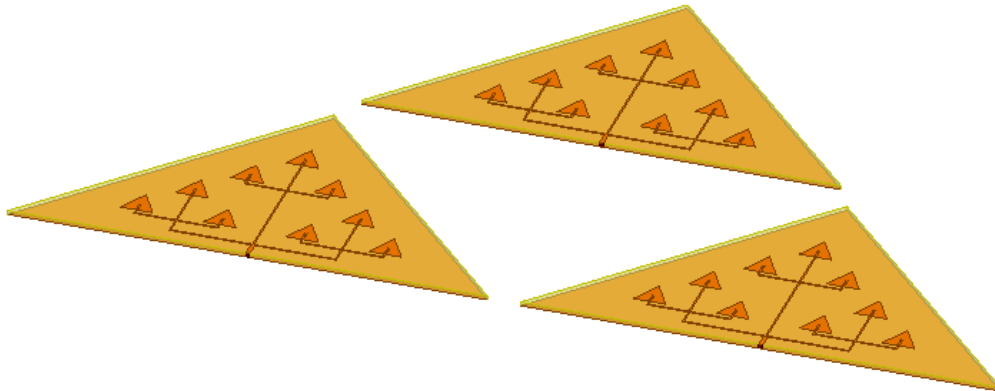


Figure 3.16. Three triangular antenna array

This antenna, shown in Fig. 3.16, has a gain of 16.52 dB, shown in Fig. 3.17. It consists of three planar triangular antenna arrays of the design shown in Fig. 2.13. The three antenna arrays are placed in the same xy-plane, all facing the positive z-plane with a spacing of 2 mm between them. This design has three input points each coming from the 50  $\Omega$  input impedance.

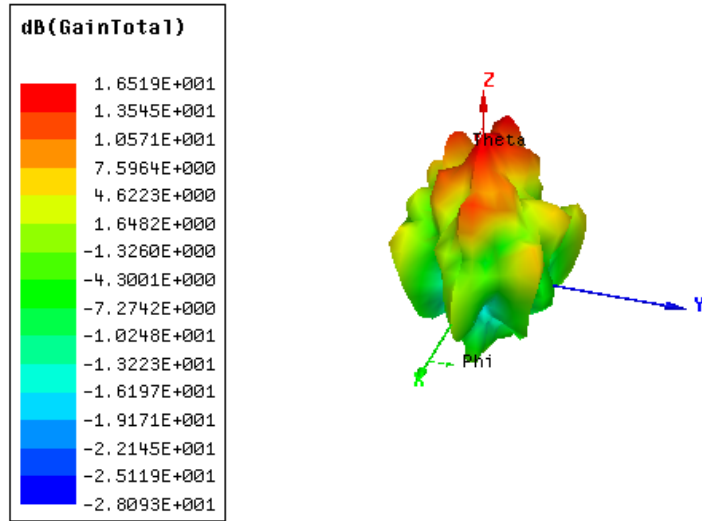


Figure 3.17. Design 1 Gain

### B. Design 2: C-shaped Curve

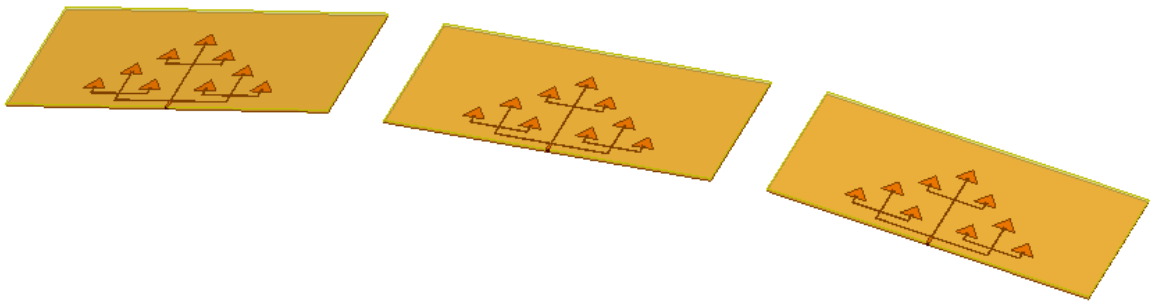


Figure 3.18. C-shaped Curve

The antenna with a gain of 14.5 dB, Fig. 3.19, is shown in Fig. 3.18. It consists of three planar antennas of the design shown in Fig. 2.10, linearly placed in the same xy-plane all facing the positive z-plane in a shape of a letter "C" but with widely-opened extremities. The antenna arrays placed at the edges are tilted by 10 degrees from the positive to the negative z-plane with a spacing of 5 mm between each two planar antennas. This design has three input points from the 50  $\Omega$  input impedances of the three planar antenna arrays.



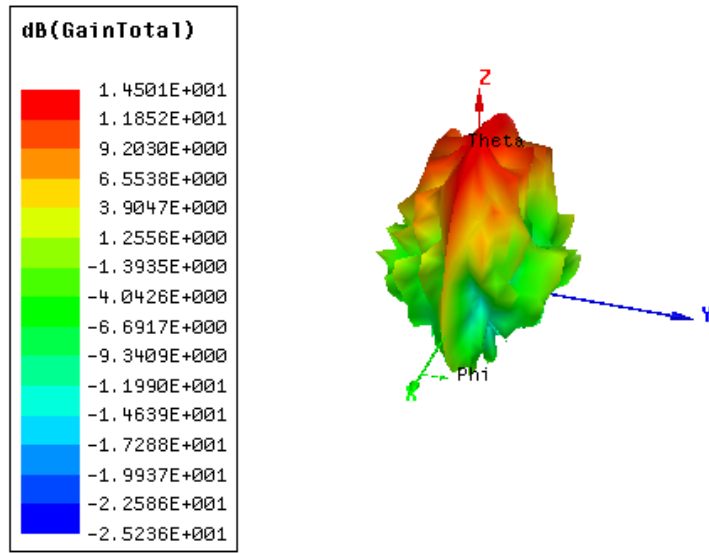


Figure 3.19. Design 2 Gain

### C. Design 3: 3D Triangle

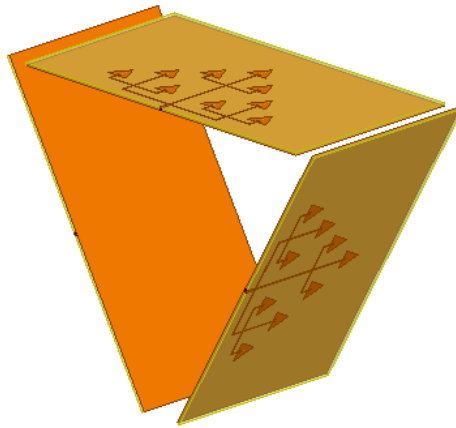


Figure 3.20. 3D Triangle

The antenna is shown in Fig. 3.20; it has a gain of 10.03dB shown in Fig. 3.21. It consists of three planar antennas of the design shown in Fig. 2.10. It resulted from the previous antenna, Fig. 3.18, however the tilt is 120 degrees instead of 10 degrees, to form a triangle. The three antenna arrays are placed like a triangle with a spacing of 2 mm between them. This design has three input points each coming from the 50  $\Omega$  input impedance.

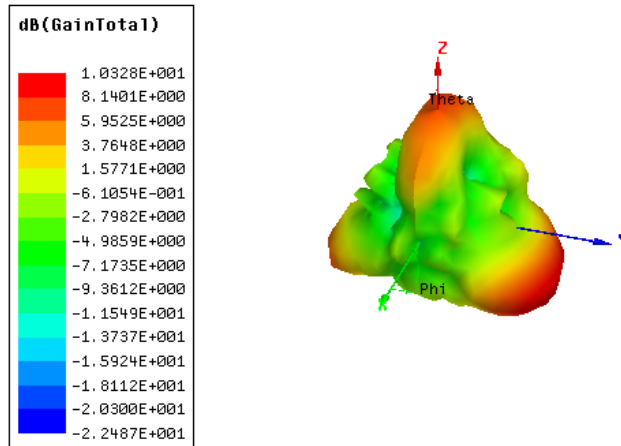


Figure 3.21. Design 3 Gain

#### D. Design 4: Triangular pyramid

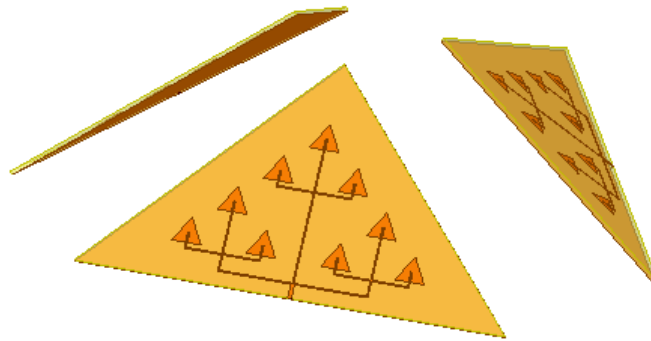


Figure 3.22. Triangular pyramid

This antenna has a gain of 9.8 dB, Fig. 3.23. Three planar triangular antenna arrays of the design shown in Fig. 2.13 are placed like a pyramid with a tilting of 45 degrees of each antenna array from the positive to the negative z-plane and with a spacing of 5 mm between each two arrays as depicted in Fig. 3.22. There are three input points coming from the 50  $\Omega$  input impedance of each antenna array.

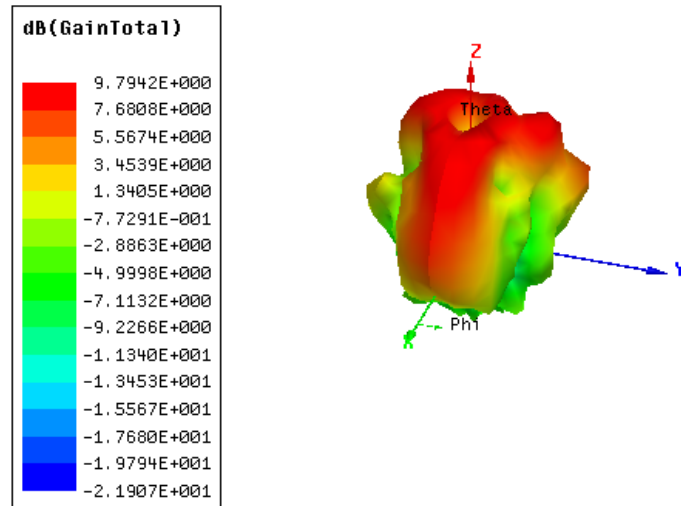


Figure 3.23. Design 4 Gain

**E. Design 5: Square pyramid**

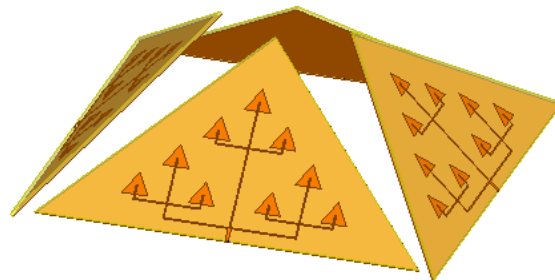


Figure 3.24. Square pyramid

This antenna has a gain of 9.41 dB, Fig. 3.25; however, it is formed of four planar triangular antenna arrays of the design shown in Fig. 2.13, placed like a square pyramid. Similar to the antenna in Fig. 3.22, each antenna array is tilted by 45 degrees from the positive to the negative z-plane and with a spacing of 5 mm between each two arrays as depicted in Fig. 3.24. There are four input points coming from the 50  $\Omega$  input impedance of each antenna array.

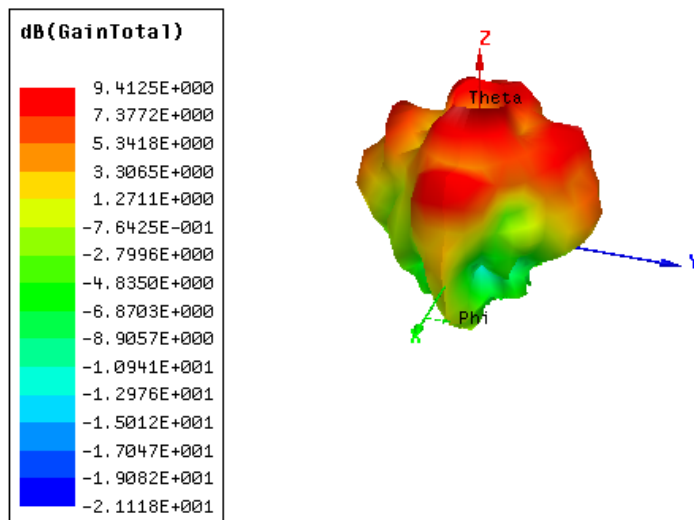


Figure 3.25. Design 5 Gain

#### F. Design 6: Crown-shaped triangular pyramid

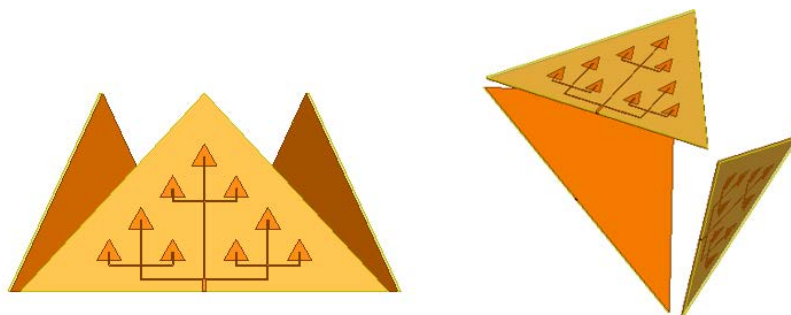


Figure 3.26. Crown-shaped triangular pyramid

The same antenna is shown in both parts of Fig. 3.26 and it has a gain of 8.41 dB as shown in Fig. 3.27. It consists of three planar triangular antenna arrays of the design shown in Fig. 2.13. The three antenna arrays are placed perpendicularly to the plane forming their base and with a spacing of 2 mm between them. This design has three input points each coming from the 50  $\Omega$  input impedance.

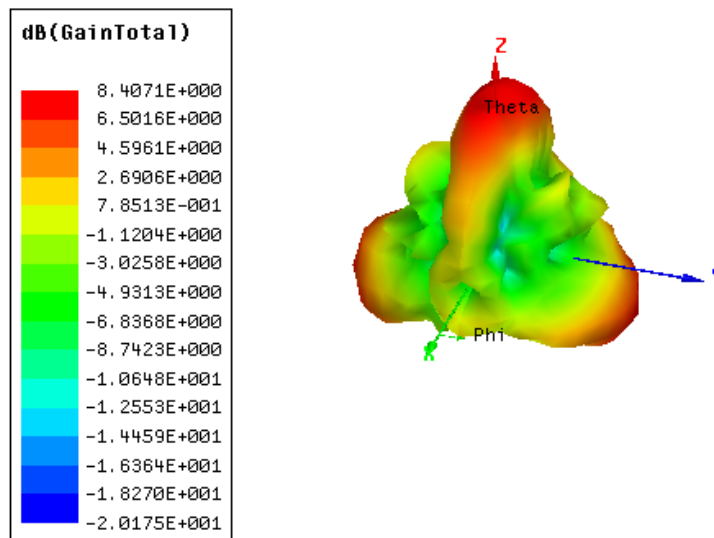


Figure 3.27. Design 6 Gain

### G. Design 7: Cube

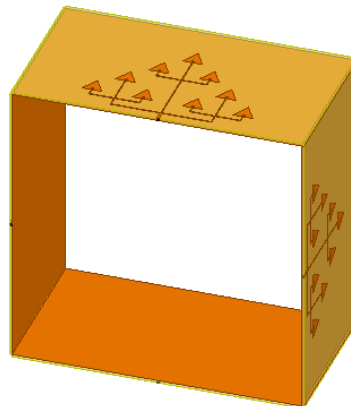


Figure 3.28. Cube

The antenna shown in Fig. 3.28, has a gain of 8.28dB, which is shown in Fig. 3.29. It consists of four planar antennas of the design shown in Fig. 2.10. The four antenna arrays are placed like a cube with no spacing between them. This design has four input points each coming from the 50  $\Omega$  input impedance.

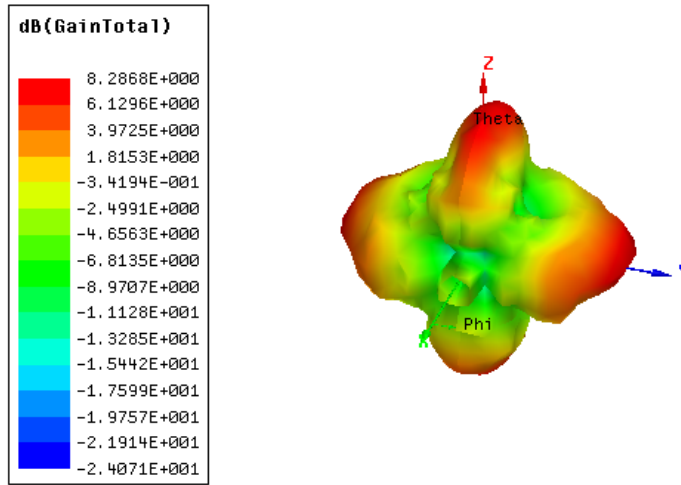
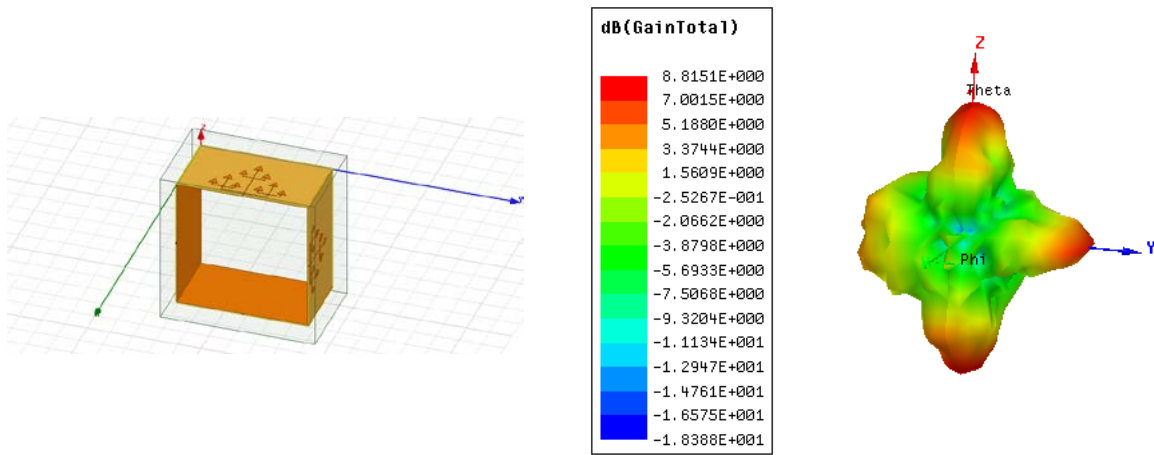
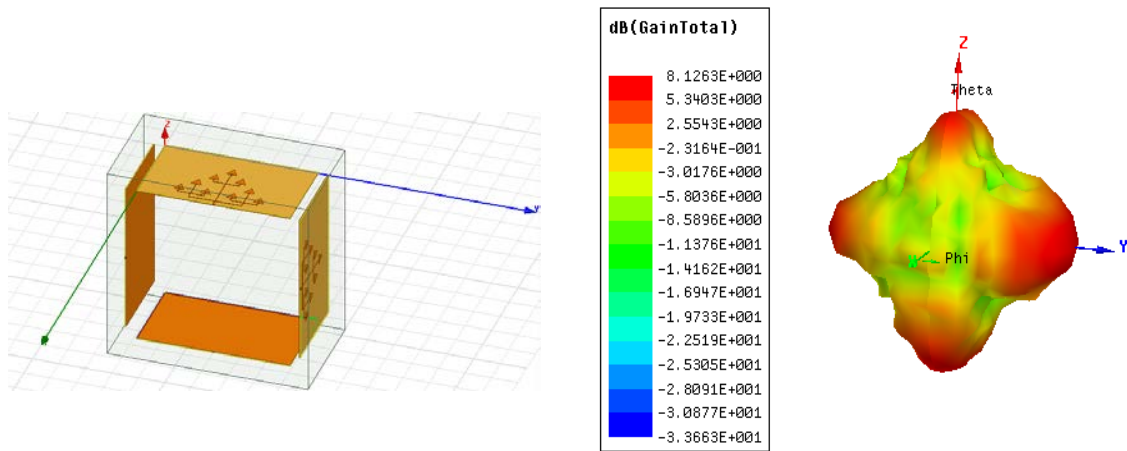


Figure 3.29. Design 7 Gain

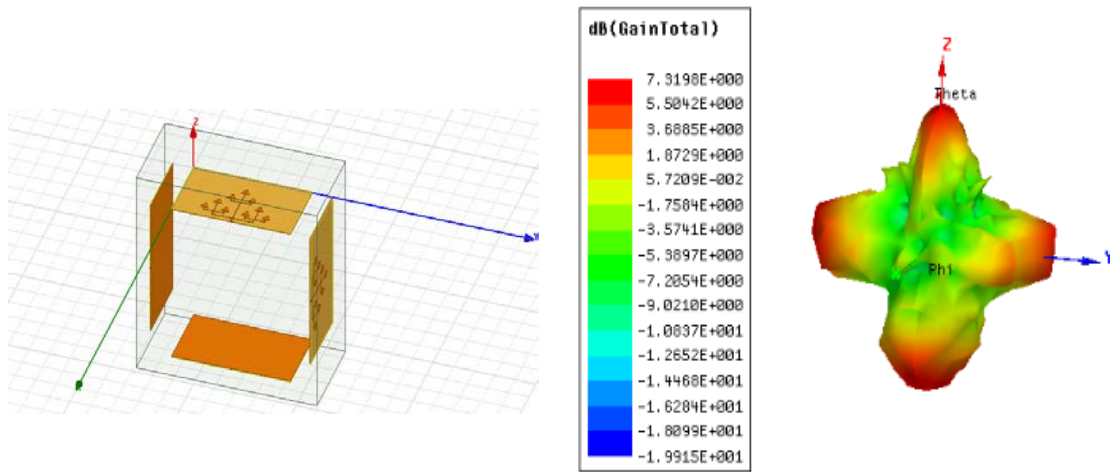
To analyze the influence of the spacing between the two-dimensional antenna arrays on the performance of the three-dimensional antenna arrays in terms of gain, a study was done on the cube-shaped antenna. In the following, Fig. 3.30, shows antennas with different spacing values and their gains. Fig. 3.30 proved that when the distance between the antenna arrays increases, the gain of the whole antenna decreases and this is due to the destructive waves resulting from the mutual coupling between the antenna arrays.



(a) No spacing



(b) Spacing = 2 mm



(c) Spacing = 5 mm

Figure 3.30. Effect of the spacing between the planar arrays

After such analysis is done on the spacing between the planes forming each one of the 3D designs, the best spacing is chosen. In the last design of chapter III, the cube with no spacing between the planes had the best gain that's why it is the one presented.



## CHAPTER IV

### RE-CONFIGURABILITY ASPECTS OF THE ANTENNAS

#### A. Frequency tunability using varactors:

Tunable antennas, [36], have two different topologies regarding the varactor connections: the first is the connection of the varactors across the patch radiating edges in parallel as in [37] and [38]. The second topology, which is the one used in this thesis, is to connect the varactors serially across a slot subtracted from the radiating patch, which means between two halves of the patch as in [39] and [40]. When comparing the two topologies, the serial connections is the preferred one in terms of the varactors value, because the fringing capacitance at the radiating edge is smaller than at the centered separation gap. Thus, for the serial connection, a higher tuning capacitance is allowed compared to the parallel when the goal is to achieve a change in the resonant frequency.

Tunability is achieved by implementing surface mounted diodes and varying their capacitance by adding a DC bias circuit. To change the capacitance of the varactors, [41], a DC bias voltage is applied and hence the frequency band will be tuned to a different frequency. According to [42], the tunability of the antenna is therefore achieved by inserting small slots cut from the transmission lines and varactors added in their place.

The diode model used here, shown in Fig. 4.32, has a length of 1 mm and it is composed of a serial connection of a capacitance and a resistor with a very small value of  $0.01 \Omega$  that has a length of 0.12 mm, which is a fraction of the 1 mm varactor model. The resistance acts as a short if modelled in parallel with capacitance, which diminishes the

capacitive or the tuning effect of the varactor, [43]. However, the capacitive effect of the varactor is retained at higher frequencies. The effect of the capacitance in series with the resistance leads to a frequency tunability in a smaller range.

The capacitance of the varactor that will be used, 1SV325, is varied between 7 pF and 80 pF when a reverse voltage between 0 V and 6 V is applied.

Fig. 4.31 represents the nine-element array with the varactors on the transmission lines preceding each patch. The obtained reflection coefficients for seven different capacitance values are shown in Fig. 4.33. Here, the frequency tunability is presented in the range [20 GHz - 35 GHz] with many additional resonances while having a consistent radiation pattern with two beams radiating in  $30^\circ$  and  $150^\circ$  directions as shown in the plot of the two-dimensional radiation patterns of Fig. 4.34.

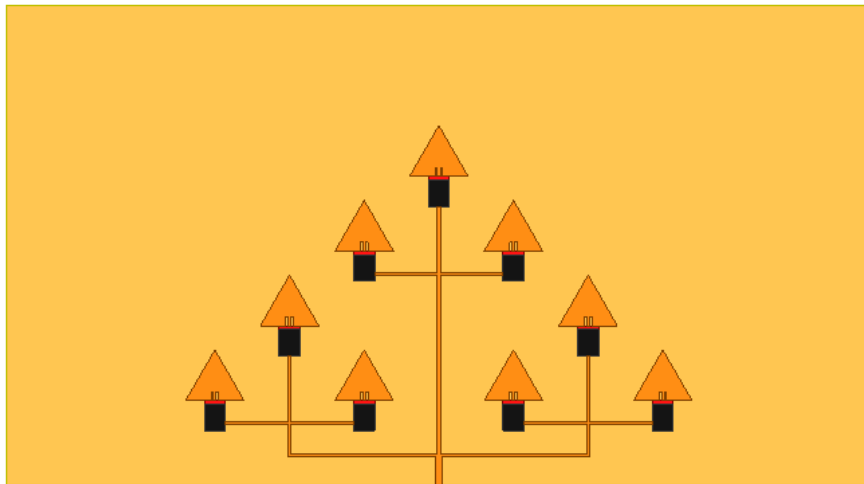


Figure 4.31: Nine-element antenna array with varactors

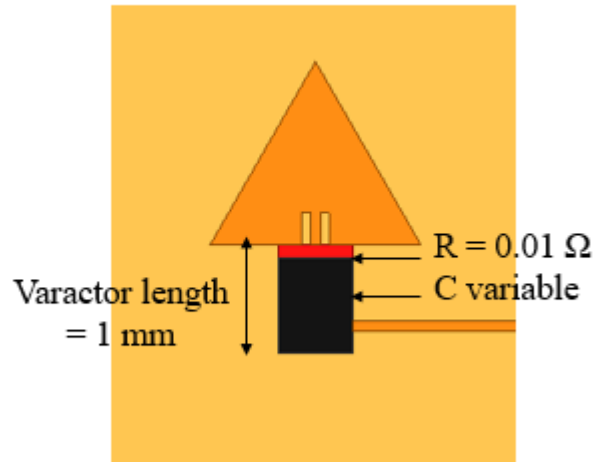


Figure 4.32. Varactor model used

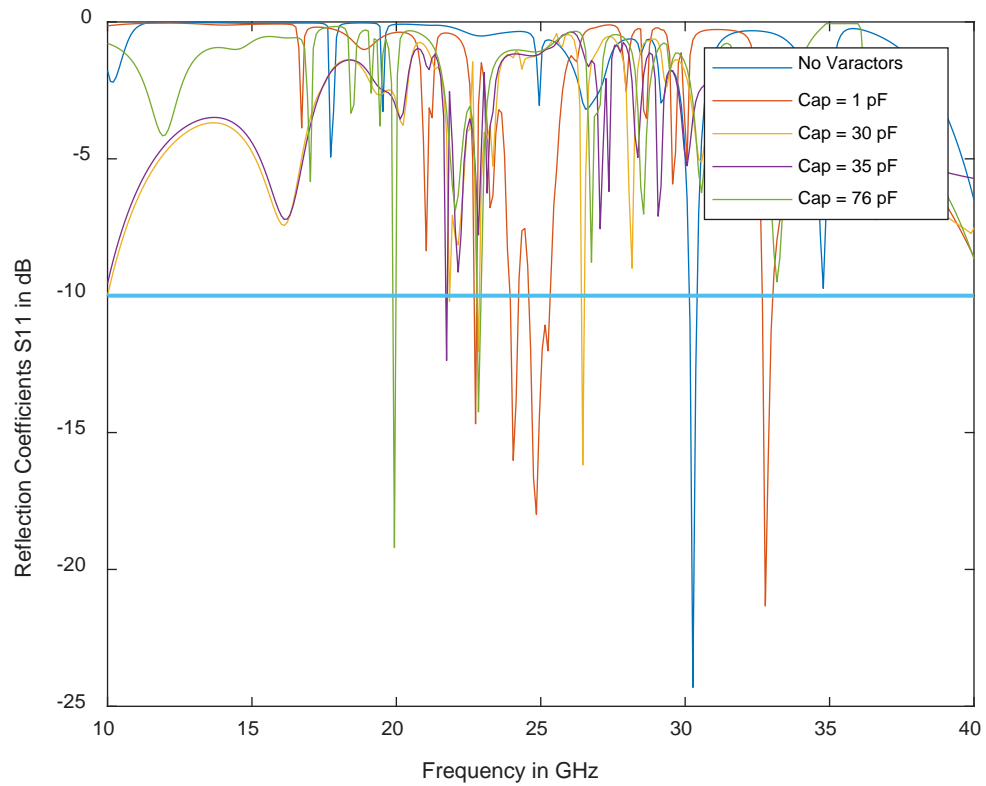


Figure 4.33. Reflection coefficients after the addition of the varactors

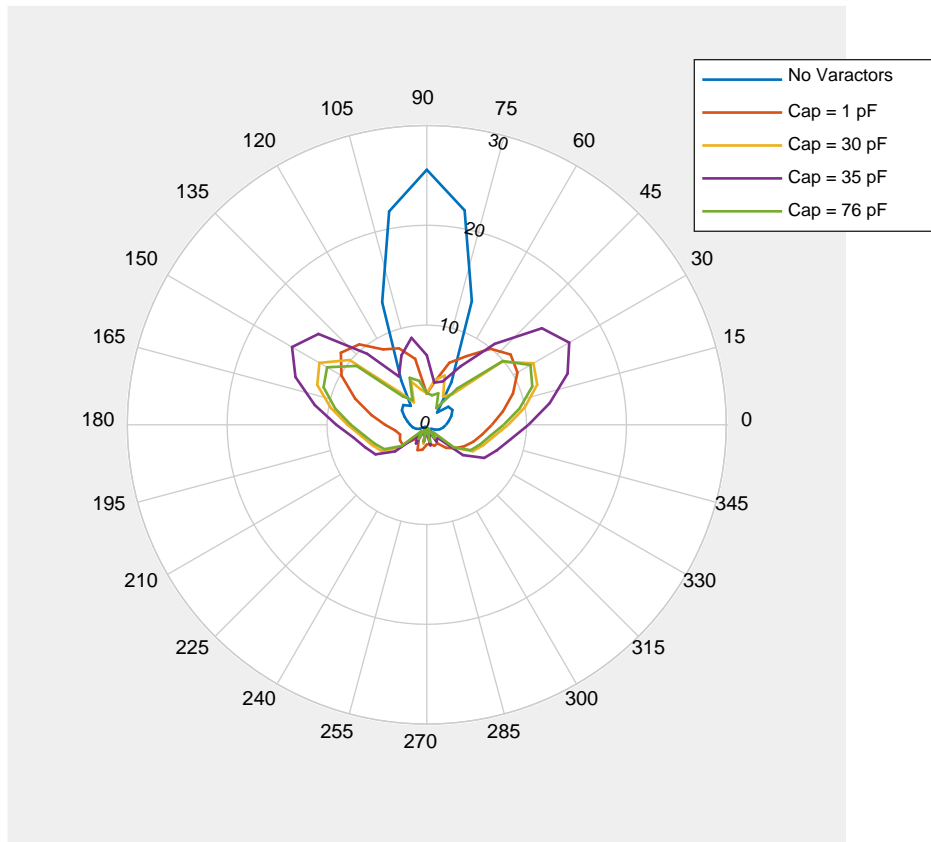


Figure 4.34. Two-dimensional radiation patterns - Varactors

According to [44], the position of the varactors obviously affect the current flow path, so to tune the obtained resonant frequency, changing these positions is a must. The positions of the varactors are selected to achieve frequency tuning while the antenna matching is kept sufficient with minimal perturbation. However, in the case of the design made in this thesis, changing the position of the varactors is hardly possible since the antennas designed have millimeter sizes with transmission lines of widths smaller than the varactor components. Therefore, the set of tunable frequencies is chosen so that a good matching condition with a low  $S_{11}$  is maintained.

The current distribution on the surface of an antenna determines the radiation pattern of the antenna and its functionality, [42]. New current paths will be created as well as new radiation edges if a slight change in the geometrical configuration of the structure occurs and the antenna will have new resonances and different operations. In our case, the antenna presented a new set of resonances, falling between 20 GHz and 35 GHz, which makes it useful for many practical applications in addition to 5G.

Directivity and beam scanning at desired angles with frequency sweep are two radiation pattern characteristics achieved by the designed antenna array after adding varactors to it. With the help of the varactors, a shift in the frequency is obtained in the previous part.

After varying the value of the capacitance between 0 pF and 80 pF while having a fixed resistance, simulations showed a very wide range of operational frequencies. Some capacitance values resulted in the same resonant frequency approximately, therefore a study on their radiation pattern had to be done. No change was observed in the radiation patterns of the antennas loaded with varactors of different capacitance values and resonating at the same frequency. Therefore, another approach had to be used to prove the beam steering capability of two antenna designs.

#### **B. Beam steering using phase shifts:**

The continued exponential growth in millimeter-wave applications has put a lot of attention on beam steerable antennas, [45], that are identified as an attractive solution for 5G communication networks. Beam switching or scanning to targeted users while suppressing unwanted signals is achieved using this type of antennas.

This approach consists of transforming the nine-element antenna array, having a single input, to a MIMO antenna with three different inputs each feeding one of the three-element patches and exciting each of these inputs with a different phase. Fig. 4.35 represents the geometry of the antenna and Fig. 4.36 represents its reflection coefficients. In the following Table 4.6, different combinations of phases are presented as sets of three angles. These combinations proved the ability of beam steering the radiation pattern of the antenna using this approach.

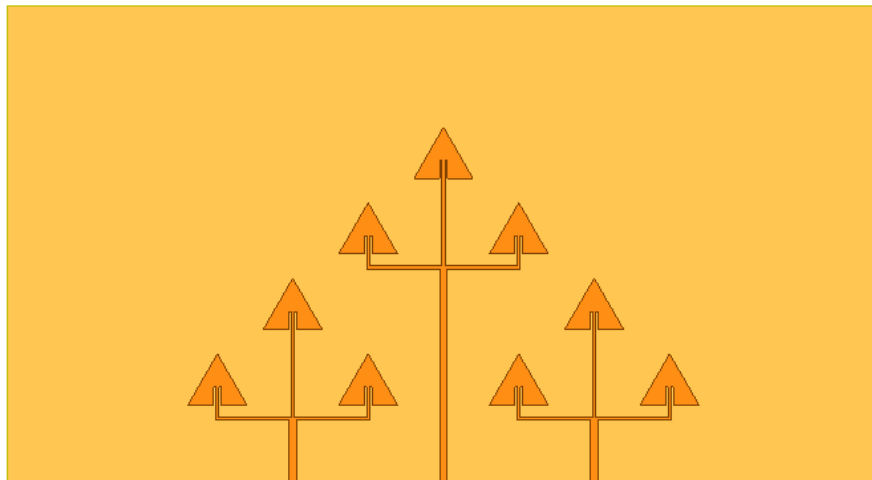


Figure 4.35. Three-input nine-element antenna array

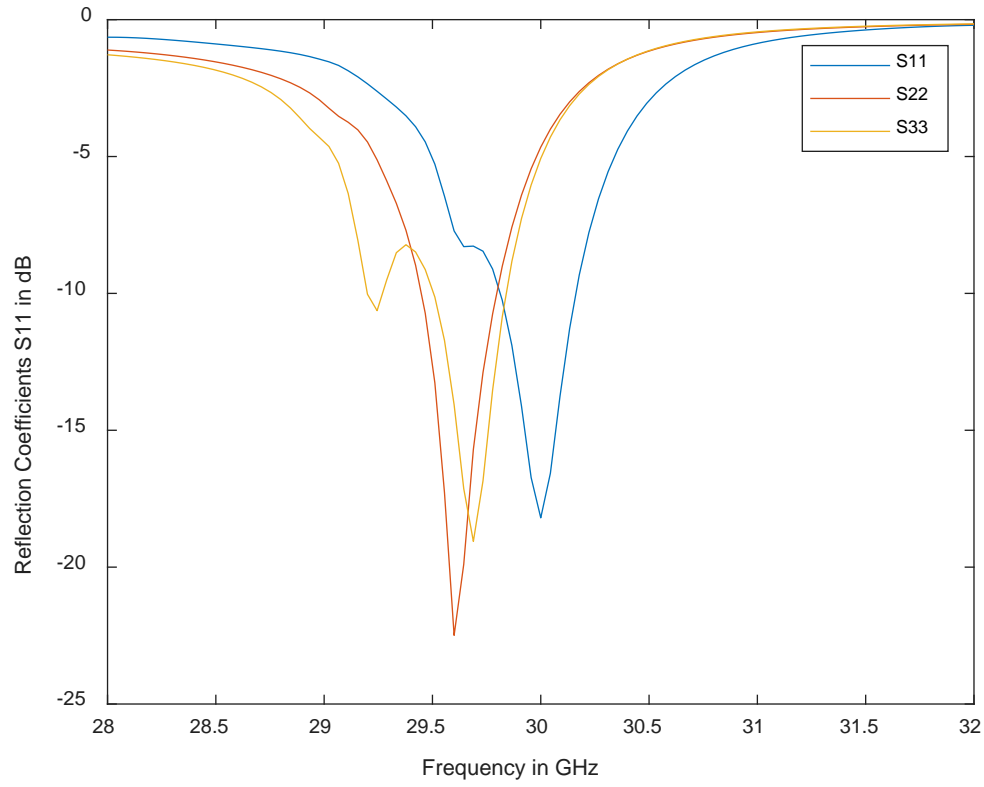
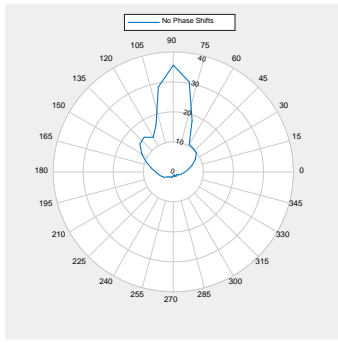


Figure 4.36. Reflection coefficients of the three-inputs nine-element antenna array

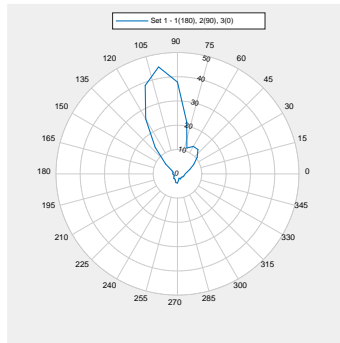
TABLE 4.6. Three phases combinations

	<i>Set 1</i>	<i>Set 2</i>	<i>Set 3</i>	<i>Set 4</i>
<i>Input 1</i>	180°	180°	0°	0°
<i>Input 2</i>	90°	0°	0°	180°
<i>Input 3</i>	0°	90°	180°	0°

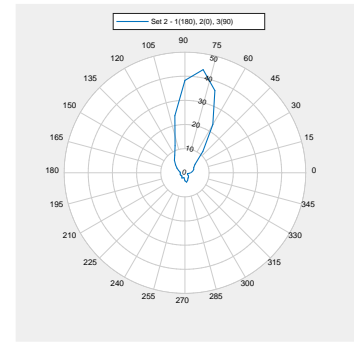
Set 1 and Set 2 tilted the beam by 10° to the right and left of the original beam, having no phased excitations. Set 3 and Set 4 tilted it by 20° to the right and left of the original beam direction as shown in Fig. 4.37.



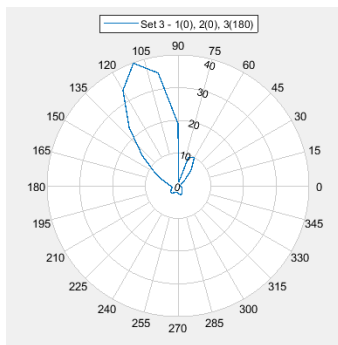
(a)



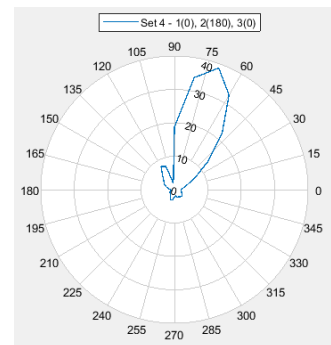
(b)



(c)



(d)



(e)

Figure 4.37. Two-dimensional radiation patterns – Phase shifts

Fig. 4.38. shows the corresponding three-dimensional radiation patterns presenting the total gain of the antenna also. A small second lobe is appearing in the 3D plots but not showing in the 2D radiation patterns and this is because it falls in a different plane. Two new coordinate systems could be created with their y-axis perpendicular to the direction of the two low level side lobes indicated by the arrows in Fig. 4.38 (a), the radiation pattern of the antenna with no phase shifting, to prove the beam steering of these lobes also using the same approach of phase shifting.



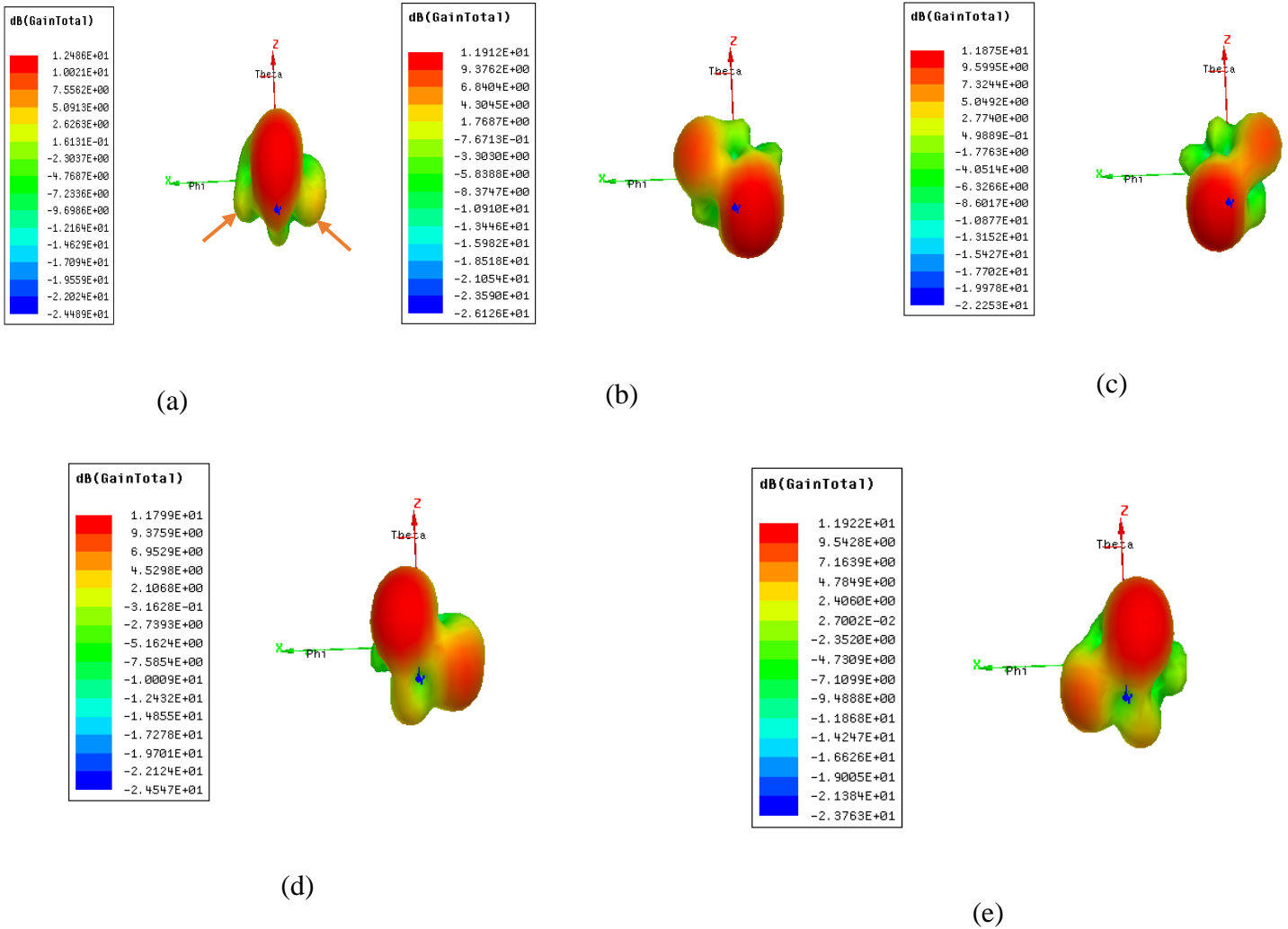
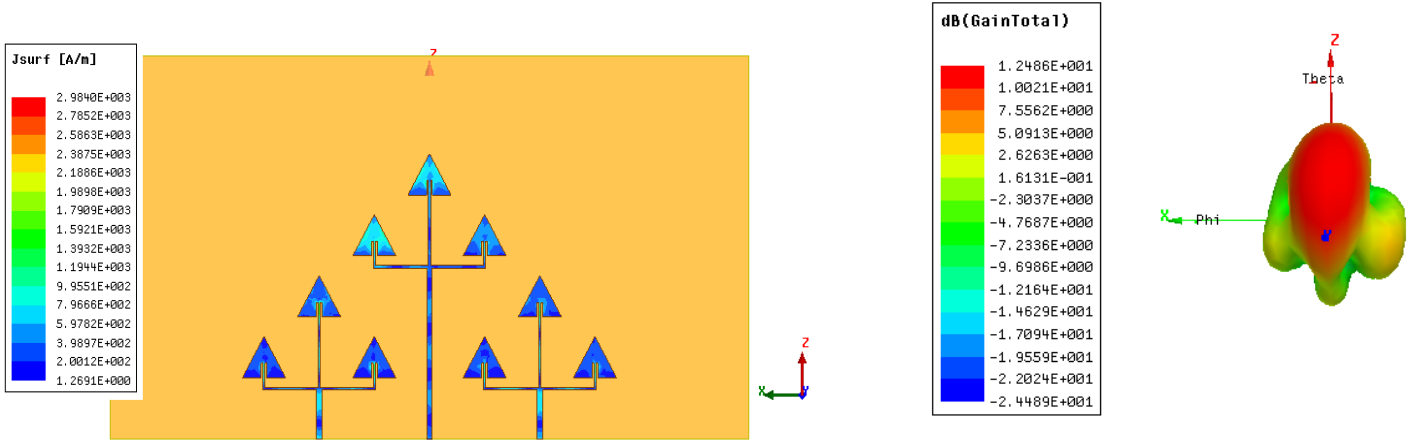


Figure 4.38. Three-dimensional radiation patterns – Phase shifts

A study was done on the current distribution of two antenna designs to check how it is related to the radiation pattern. Fig. 4.39. (a), shows the current distribution on the patches of this MIMO antenna and Fig 4.39. (b), shows its 3D radiation pattern plot. In the two lower generators the current is less than the current propagating in the top-centered generator. Also not can be noticed that the edges of the inset feed gap exhibits higher current propagation than the rest of the patch and this may be due to the fringing fields at the edges.



(a) Current distribution

(b) 3D Radiation pattern

Figure 4.39. Three inputs MIMO antenna

After removing the top-centered generator and keeping only the two generators placed horizontally, a study was done on the current propagation in the patches of this MIMO antenna design and its radiation pattern, as shown in Fig. 4.40. From Fig. 4.40. (a), it is shown that the current is distributed in a similar way in the two generators because they have similar geometries. The 3D radiation pattern shown in Fig. 4.40. (b), is now spread along the z-axis; radiation is now less directive to the top since the top generator is removed and obviously the gain decreased for the same reason.

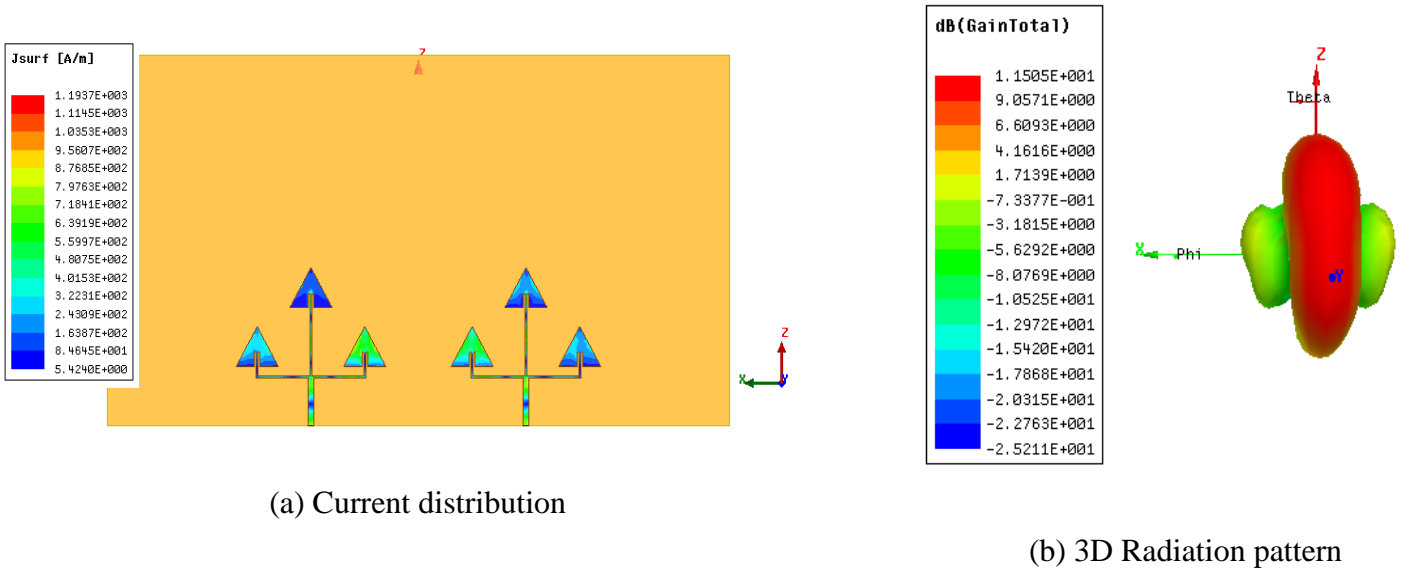


Figure 4.40. Two inputs MIMO antenna

The gain of the three inputs MIMO antenna could be further increased by enlarging the space between the middle and the two sided generator elements; this space could be doubled or increased by a quarter wavelength. Also the spacing from the edges will affect the results of the gain. A parametric study on these parameters could be done to achieve a better gain for this antenna design.

### C. Beam steering by mechanical rotation:

The mechanical rotation is a process that could be used to prove the ability of steering the beam of one of the 3D antennas. The study is done on the triangular pyramid antenna with no spacing between the planes.

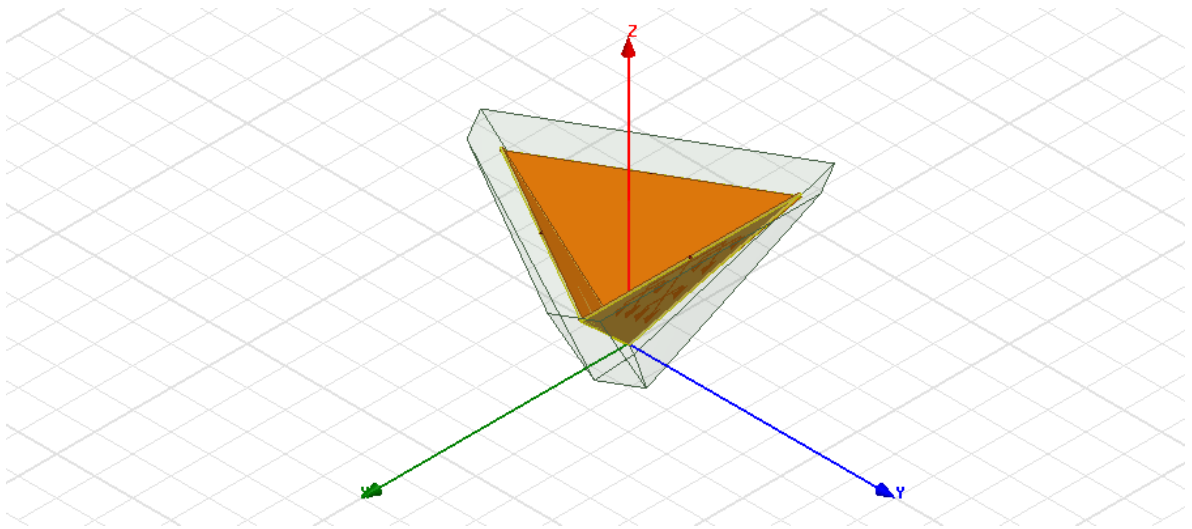
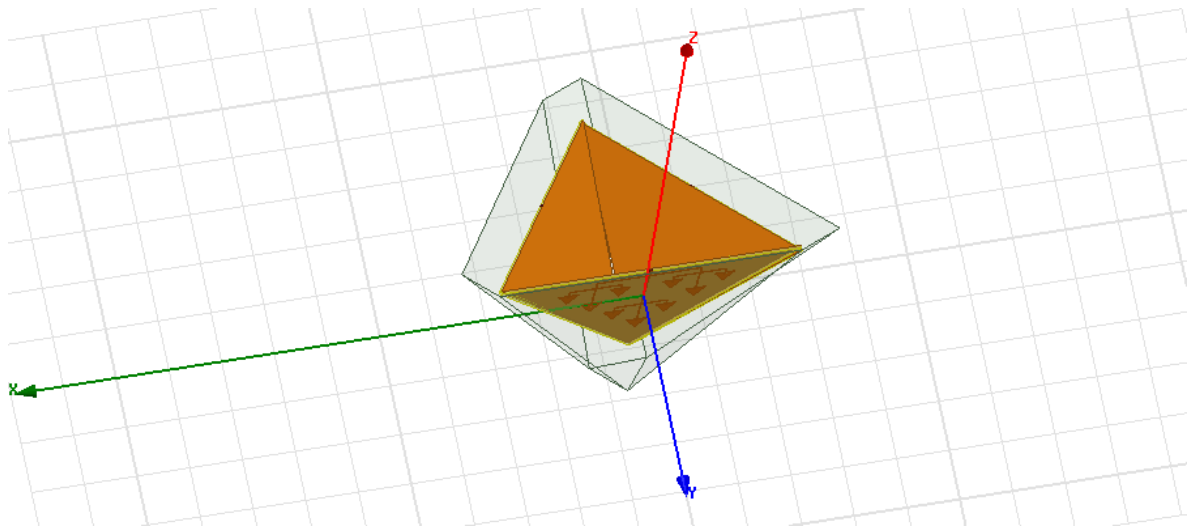
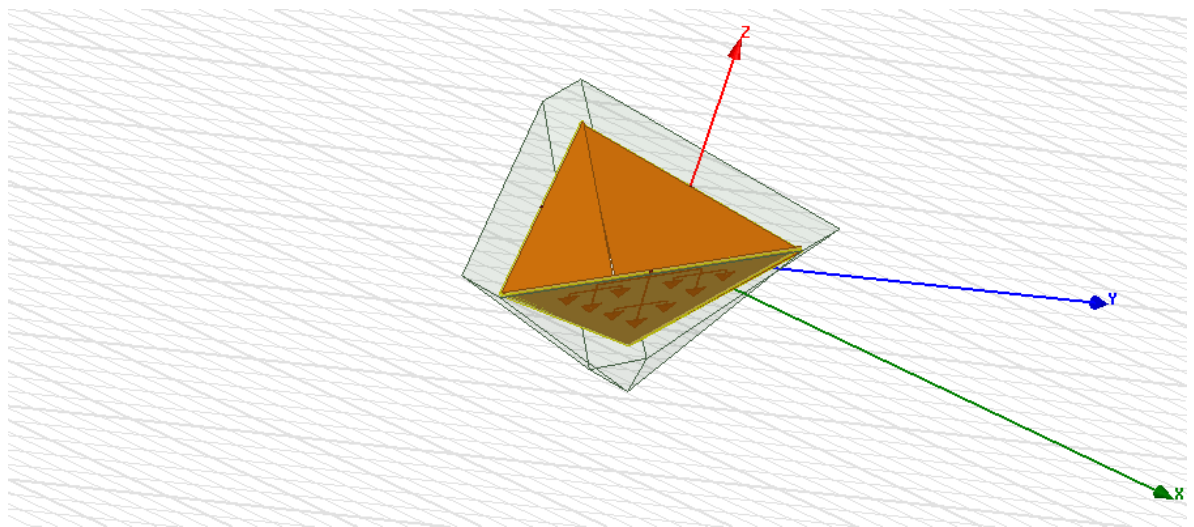


Figure 4.41. Rotational coordinate system of the 3D triangular pyramid

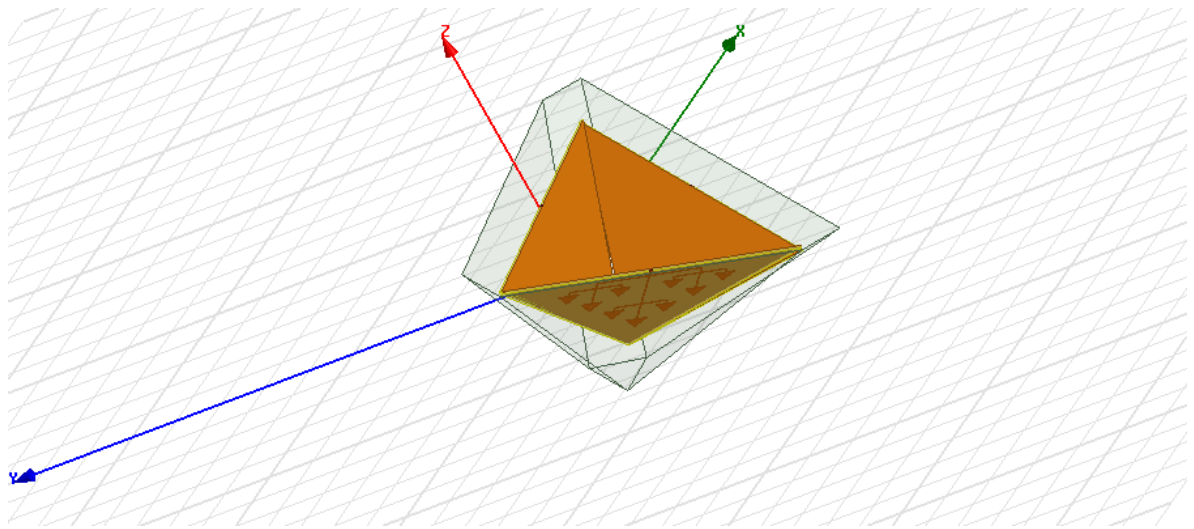
The antenna, in this part, is supposed to be rotating around a fixed z-axis attached to it from its bottom, the pyramid being placed upside down as shown in Fig. 4.41. Three different coordinate systems were created as shown in Fig. 4.42, to check the radiation pattern of each array plane independently from the other; however, the simulation were done on one coordinate system since all of the three are supposed to have symmetrical characteristics. Figs. 4.43 and 4.44 shows that the radiation pattern is being steered when the antenna is rotating.



(a) Coordinate System 1

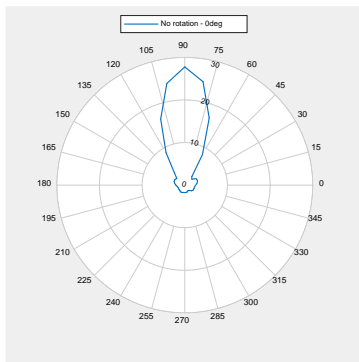


(b) Coordinate System 2

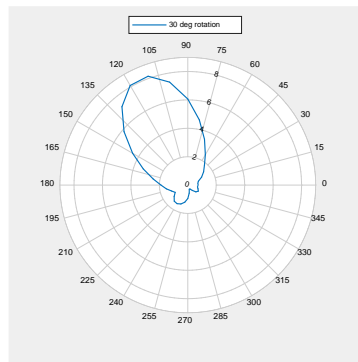


(c) Coordinate System 3

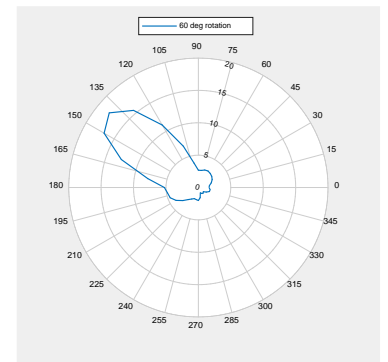
Figure 4.42. Coordinate systems for the radiation pattern of each triangular plane



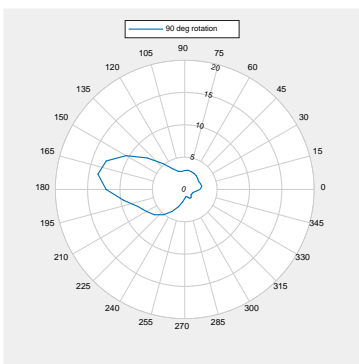
(a) No rotation -  $0^\circ$



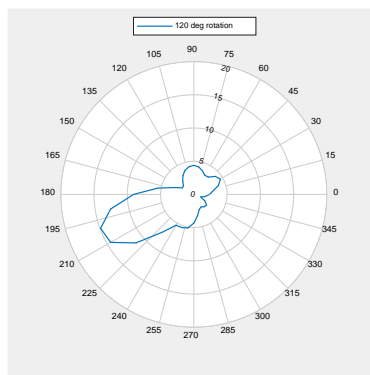
(b)  $30^\circ$  rotation



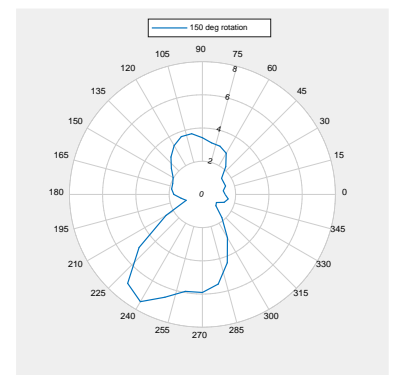
(c)  $60^\circ$  rotation



(d)  $90^\circ$  rotation

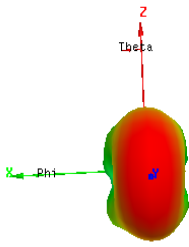
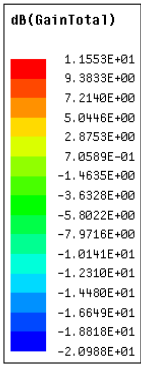


(e)  $120^\circ$  rotation

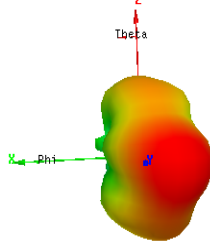
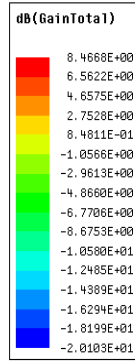


(f)  $150^\circ$  rotation

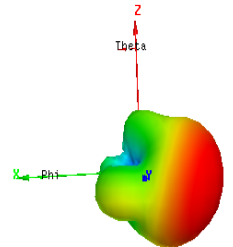
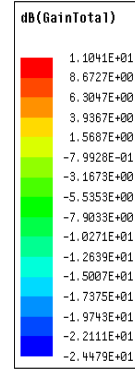
Figure 4.43. Two-dimensional radiation patterns – Mechanical rotation



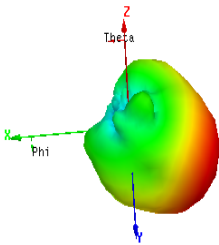
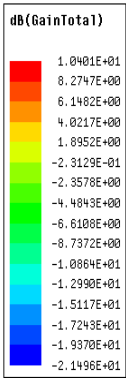
(a) No rotation - 0°



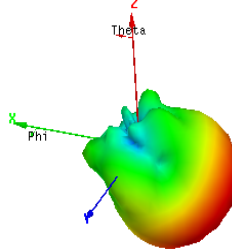
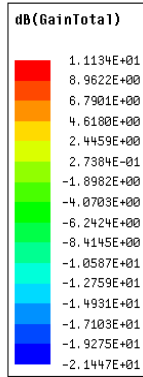
(b) 30° rotation



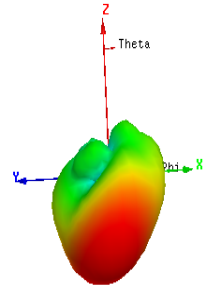
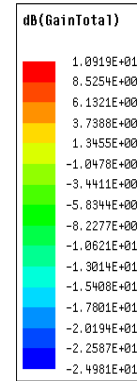
(c) 60° rotation



(d) 90° rotation



(e) 120° rotation



(f) 150° rotation

Figure 4.44. Three-dimensional radiation patterns – Mechanical rotation

## CHAPTER V

### CONCLUSION

In [46], it is stated that future cellular communication networks induced the exploration of the underutilized millimeter wave frequency spectrum because of the global bandwidth shortage facing wireless carriers. Some resulted measurements presented in [46], shows that these frequencies can be used when employing steerable and directional antennas in base stations and mobile devices.

Wireless service providers are facing a big challenge to overcome the global bandwidth shortage caused by the rapid increase of mobile data growth and the use of smartphones. The ever-growing consumer data rate demands has to be supported by the mobile broadband networks that needs to tackle the exponential increase in the predicted traffic volumes. Wireless carriers must be prepared to support a large increase in the total mobile traffic since the demand for capacity is increasing dramatically every year.

The main difference between the fourth generation networks and 5G is that fifth generation uses much greater spectrum allocations at untapped millimeter wave frequency bands as well as highly directional and beamforming antennas at both the base station and the mobile device. Other features may include longer battery life, lower outage probability, much higher bit rates in larger portions of the coverage area, lower infrastructure costs, and higher aggregate capacity for many simultaneous users in both licensed and unlicensed spectra similar to the convergence of Wi-Fi and cellular, as stated in [46]. Millimeter wave



wireless connections are the backbone networks of 5G, which will allow rapid positioning and mesh-like connectivity with collaboration between base stations.

Since wireless communication systems are being developed rapidly, [47], a wide interest for low cost and high data rates appeared. 5G wireless systems have multiple challenging demands, [48], one of which is the availability of the bandwidth; to accomplish this demand, millimeter wave bands are intentionally used by future wireless networks. 30 GHz is here emphasized for 5G because, compared to other millimeter wave frequencies, it has lower atmospheric absorptions and attenuations. According to [49], unprecedented bandwidth and opportunities is provided by millimeter waves of frequency between 30 GHz and 300 GHz for new applications and high data rate wireless applications.

In millimeter wave applications, [50], the weight and the volume of the antenna have to be kept minimum and in these applications conformal microstrip antenna arrays are needed. Therefore, printed antennas are promising candidates for such applications. However, ohmic and dielectric losses in the feed network of these antennas degrade the efficiency of printed arrays and it is all due to the parasitic radiation in their feed network as well as the excitation of surface waves in the dielectric substrate. Large arrays containing long and complicated feed networks exhibits the most severe efficiency limitations and that is also due to the high frequencies where the dielectric and the ohmic losses are high.

Some of the factors that may attribute to the performance degradation is the fact that the antenna array as well as the transmission lines are both etched on the same layer, [51], which reduces the manufacturing cost however, some signals may be radiated or received by the transmission lines and that will increase the side lobe level and cause a

decrease in the efficiency of the antenna. A solution to this problem could be to design antennas printed on multiple layers. The antenna feeding network will be on a plane separated from the plane of the antenna radiating elements by an air gap, which will reduce the spurious effects caused by the transmission feed line.

New and innovative antennas have to be created to further improve modern communication system technology and overcome the recently faced problems, [35]; therefore, researchers are studying many different approaches and techniques. One of these techniques has involved combining aspects of antenna design with the modern theory of fractal geometry. This so called fractal antenna engineering, is a growing area of research that received a lot of recent attention.

In addition, modern telecommunications demand miniaturized antennas operating over multiple bands, [44], which force antenna designers to research for ways to improve the antenna characteristics. Many services have to be grouped in an increasingly narrow space so the fractal antenna design is a research hotspot for the solution of this issue. Fractal shapes are based on self-repetition and a fractal-shaped antenna employs the self-similarity property to maintain its characteristics.

Microstrip patch antennas have an important limitation, and that is the narrow impedance bandwidth they provide, which is of the order of few percent, [52]. In recent years, several techniques have been studied and proposed to overcome this problem and improve this bandwidth. Some of these techniques are using matching structures, using a parasitic patch or using a substrate having a low dielectric constant. The improvement of the effective bandwidth could be achieved by implementing varactor diodes in the

microstrip patch, [38] and [53]. This is presented by multiband antennas, [41], that have been proposed to serve the purpose of integrating as many standards as possible into a single wireless device caused by the development of many different wireless communications standards.

Different wireless networks operating on different radio frequency bands are required by the latest and next generation mobile radio terminals, [54], to have an effective operation, these terminals need either a wideband antenna that operates on the entire useful mobile frequencies or an antenna that could be tuned to operate on the required relatively narrow bands when desirable. So antenna designers are facing an additional challenge imposed by the large bandwidth needed for multimedia services that operate over multiple frequency bands. Tunable antennas could be either achieved by adding varactor diodes to their design for continuous tuning, [55], or by creating a switching system using either pin diodes [56] or MEMS [57].

In the case of frequency re-configurability, [58], the high gain and the radiation pattern characteristics could be maintained. The implementation of semiconductor devices, for example, pin diodes and varactors, were easily done on microstrip antennas thanks to their minimal dissipation as well as their millimeter sizes. Frequency re-configurability could be achieved by using pin diodes because they are mainly used in switching 'ON' and 'OFF'. However, varactor diodes have a capacitive load that is subject to change under controlled reverse voltage of up to 30 V. Thereby, the electrical length of the RF signal that travels through the antenna will be varied when adding varactors along the current path and that will result in a shift in the frequency.

New characteristics could be added to existing designs when mounting varactors on them such as achieving a tunable antenna with fixed radiation pattern characteristics or beam scanning along with frequency tunability or beam steering while having a fixed resonant frequency. Obviously, a resistance in parallel to the capacitor in the varactor model draws the current through the resistor and minimizes the influence of the variable capacitance, [43], but when the resistance has a large value the capacitive nature is retained. For frequency tuning of microstrip antennas it is preferred to use a purely capacitive load; however, if the capacitance of the varactor model is in series to a resistor, a special care should be taken when choosing the value of the resistance. The frequency is determined by the antenna dimensions and the value of the capacitance, [25], so choosing the proper capacitor value tunes the frequency. Moreover, if a varactor is used with a biasing network, the electronic tuning is attained by changing the applied DC voltage.

The development of pattern re-configurable antennas is driven by the recent demand of compact wireless devices, [36]. These antennas are capable of changing their main beam direction whereas conventional antennas have fixed radiation pattern. This feature results in the ability to avoid noisy environment and to strengthen the signal detection from an intended target. Previously, beam steering was realized with phased arrays. However, since compactness and low cost of the antenna terminals is an important necessity, large phased arrays could be an eliminated approach. Recently, continuous beam scanning achieved by loading the antenna with varactors is used instead of discrete beam switching.

Reconfigurable antennas, [59], could be used in communications, electronic surveillance and electronic counter measures that's why they have received significant attention recently. Their properties could be adapted to achieve selectivity in frequency and beam direction. Therefore, compared to broadband antennas and antennas with fixed radiation patterns, these antennas offer the advantages of compact size, efficient use of electromagnetic spectrum and frequency selectivity. The adverse effects of interference and jamming could be reduced by frequency selectivity.

In this thesis work, the millimeter wave antennas were optimized to meet multiple requirements with a minimum tradeoff between their characteristics. These antennas have a reduced size to fit in handheld devices, a sufficient bandwidth, a high directivity, beamforming capability to be able to perform spatial scanning and a reflection coefficient less than -6 dB, which is the acceptable threshold for operation in the mobile antenna standards. The shape of the patches is chosen to be triangular not only for the novelty of the designs made to operate at millimeter waves, but for the better performance in terms of low side lobe levels already proven in the literature. A substrate of aluminum oxide was used because it has a high dielectric constant, which helps meeting the requirements of reduced size and millimeter wave frequency operation of these antennas. A third dimension was added to antenna arrays to improve more their performance and increase their gain. Finally, varactors were added to provide the beam steering as well as the frequency tuning capability of the antenna.

Multiple two-dimensional and multi-faceted three-dimensional antenna designs are presented in this thesis. The antennas having good gain, could be good candidates for use at

millimeter waves and 5G since they present good performance in terms of small size, low reflection coefficient, high gain and beam scanning capability. These antennas could be used embedded in handheld devices thanks to their light-weight and small size. However, fabrication and measurement of these antennas in Lebanon is almost impossible because of their high operational frequency leading to a very small size, as well as the unavailability of the ceramic substrate used. A research was done on some international companies that could fabricate these antennas and also measure their reflection coefficients and their radiation patterns. Finally, the job could be done by Rennes University laboratories in the summer.

## BIBLIOGRAPHY

- [1] M. R. Bhalla and A. V. Bhalla, "Generations of Mobile Wireless Technology: A survey," *International Journal of Computer Applications*, vol. 5, no. 4, pp. 26-32, August 2010.
- [2] A. Nordum, "Everything you need to know about 5G," 27 January 2017. [Online]. Available: <https://spectrum.ieee.org/video/telecom/wireless/everything-you-need-to-know-about-5g>. [Accessed 18 September 2017].
- [3] N. Lahoria, S. B. Rana and N. Kumar, "5G Future Communication: Requirements and Challenges," in *47 Mid-Term Symposium on Modern Information and Communication Technologies for Digital India*, India, 2016.
- [4] A. Sebal, "High Gain Millimeter Wave Antennas for 5G Wireless and Security Imaging Systems," in *33rd National Radio Science Conference*, Aswan, Egypt, 2016.
- [5] M. El Shorbagy, R. M. Shubair, M. I. Al Hajri and N. K. Mallat, "On the Design of Millimeter-Wave Antennas for 5G," in *16th Mediterranean Microwave Symposium*, Abu Dhabi, United Arab Emirates, 2016.
- [6] D. A. Outerelo, A. V. Alejos, M. G. Sanchez and M. V. Isasa, "Microstrip Antenna for 5G Broadband Communications: Overview of Design Issues," in *IEEE International Symposium on Antennas and Propagation & USNC/URSI National Radio Science Meeting*, Vancouver, BC, Canada, 2015.
- [7] A. El-Bacha and R. Sarkis, "Design of Tilted Taper Slot Antenna for 5G Base Station Antenna Circular Array," in *IEEE Middle East Conference on Antennas and Propagation*, Beirut, Lebanon, 2016.
- [8] A. Majumder, "Rectangular Microstrip Patch Antenna Using Coaxial Probe Feeding Technique to Operate in S-Band," *International Journal of Engineering Trends and Technology*, vol. 4, no. 4, pp. 1206-1209, April 2013.
- [9] A. M. Jajere, "Millimeter Wave Patch Antenna Design - Antenna for Future 5G Applications," *International Journal of Engineering Research & Technology*, vol. 6, no. 2, pp. 289-291, February 2017.
- [10] Y. S. H. Khraisat and M. M. Olaimat, "Comparison Between Rectangular and Triangular Patch Antennas Array," in *19th International Conference on Telecommunications (ICT 20120)*, Jounieh, Lebanon, 2012.

- [11] H. Sajjad, W. T. Sethi, K. Zeb and A. Mairaj, "Microstrip Patch Antenna Array at 3.8 GHz for WiMax and UAV Applications," in *International Workshop Antenna Technology: "Small Antennas, Novel EM Structures and Materials, and Applications"*, Sydney, NSW, Australia, 2014.
- [12] M. S. Sharawi, S. K. Podilchak, M. T. Hussain and Y. M. M. Antar, "Dielectric resonator based MIMO antenna system enabling millimeter-wave mobile devices," *IET Microwaves, Antennas & Propagation*, vol. 11, no. 2, pp. 287-293, 29 January 2017.
- [13] C.-F. Yang, C.-Y. Hsieh and C.-M. Cheng, "Design Small-Size and Wide-Band T-Shaped Patch Antenna on Ceramic Substrate," in *IEEE Wireless Communications and Networking Conference*, Kowloon, China, 2007.
- [14] M. H. Ullah, M. T. Islam, J. S. Mandeep and N. Misran, "Design and Analysis of a Multi Band Electrically Small Antenna Using Ceramic Material Substrate," *Przeglad Elektrotechniczny*, pp. 271-273, 2013.
- [15] A. Yadav and D. K. Pahwa, "Design & Parametric Study of Rectangular Slot Microstrip Patch Antenna for UWB Applications," *International Journal of Electrical and Electronics Engineering*, vol. 1, no. 3, pp. 4-7, 2014.
- [16] E. Yaacoub, M. Hussein and H. Ghaziri, "An Overview of Research Topics and Challenges for 5G Massive MIMO Antennas," in *IEEE Middle East Conference on Antennas and Propagation*, Beirut, Lebanon, 2016.
- [17] D. A. Huebener, "Directivity Characteristics of 3-Dimensional Antennas," in *Antennas and Propagation Society International Symposium*, Vancouver, Canada, 1985.
- [18] H. Aliakbari, A. Abdipour, A. Costanzo, D. Masotti and R. Mirzavand, "ANN-based design of a versatile millimeter-wave slotted patch multi-antenna configuration for 5G scenarios," *IET Microwaves, Antennas and Propagation*, vol. 11, no. 9, pp. 1288-1295, 2017.
- [19] V. R. Ekke and P. L. Zade, "Design and Implementation of T-Junction Triangular Microstrip Patch Antenna Array for Wireless Applications," *International Journal of Engineering and Technology*, vol. 8, no. 5, pp. 2105-2114, November 2016.
- [20] N. Ojaroudiparchin, M. Shen and G. F. Pedersen, "Design of Vivaldi Antenna Array with End-Fire Beam-Steering Function for 5G Mobile Terminals," in *23rd Telecommunications Forum Telfor*, Belgrade, Serbia, 2015.
- [21] R. Parolari, M. Gallo, A. P. Filisan, D. Zamberlan, V. Franchina, A. Michel and P. Nepa, "A Novel 3D Antenna for LTE MIMO Systems," in *International Conference of*



*Electrical and Electronic Technologies for Automotive*, Torino, Italy, 2017.

- [22] P. Sravani and M. Rao, "Design of 3D Antennas for 24 GHz ISM Band Applications," in *28th International Conference on VLSI Design*, Bangalore, India, 2015.
- [23] H. Anand and A. Kumar, "Design of Frequency-Reconfigurable Microstrip Patch Antenna," in *6th IEEE International Conference on Industrial and Information Systems*, Kandy, Sri Lanka, 2011.
- [24] M. S. Nishamol, C. K. Aanandan, M. P. and V. K., "Dual Frequency Reconfigurable Microstrip Antenna using Varactor Diodes," in *XXXth URSI General Assembly and Scientific Symposium*, Istanbul, Turkey, 2011.
- [25] A. Khidre, F. Yang and A. Z. Elsherbeni, "A Patch Antenna with a Varactor-Loaded Slot for Reconfigurable Dual-Band Operation," *IEEE Transactions on Antennas and Propagation*, vol. 63, no. 2, pp. 755-760, 02 December 2014.
- [26] D. Peroulis, K. Sarabandi and L. P. B. Katehi, "Design of reconfigurable slot antennas," *IEEE Transactions on Antennas and Propagation*, vol. 53, no. 2, pp. 645-654, 07 February 2005.
- [27] N. Behdad and K. Sarabandi, "Dual-band reconfigurable antenna with a very wide tunability range," *IEEE Transactions on Antennas and Propagation*, vol. 54, no. 2, pp. 409-416, 06 February 2006.
- [28] C.-H. Hu, T.-R. Chen, J.-F. Wu and J.-S. Row, "Reconfigurable microstrip antenna with polarisation diversity and frequency agility," *Electronics Letters*, vol. 43, no. 24, p. 1329, 04 December 2007.
- [29] B. Babakhani and S. K. Sharma, "Investigations on Frequency Agile Microstrip Patch Antenna Loaded with Varactor Diode," in *IEEE Antennas and Propagation Society International Symposium*, Orlando, FL, USA, 2013.
- [30] J. T. Aberle, S.-H. Oh, D. T. Auckland and S. D. Rogers, "Reconfigurable antennas for wireless devices," *IEEE Antennas and Propagation Magazine*, vol. 45, no. 6, pp. 148-154, December 2003.
- [31] D. E. Anagnostu, G. Zheng, M. T. Chryssomallis, J. C. Lyke, G. E. Ponchak, J. Papapolymerou and C. G. Christodoulou, "Design, fabrication, and measurements of an RF-MEMS-based self-similar reconfigurable antenna," *IEEE Transactions on Antennas and Propagation*, vol. 54, no. 2, pp. 422-432, 06 February 2006.
- [32] "RF MEMS reconfigurable triangular patch antenna," in *IEEE Antennas and*

*Propagation Society International Symposium*, Washington, DC, USA, 2005.

- [33] Y.-h. Yu and C.-P. Ji, "Research of Fractal Technology in the Design of Multi-frequency Antenna," in *China-Japan Joint Microwave Conference Proceedings*, Hangzhou, China, 2011.
- [34] M. A. Madi, M. Al-Husseini, A. H. Ramadan, K. Y. Kabalan and A. El-Hajj, "A Reconfigurable Cedar-Shaped Microstrip Antenna for Wireless Applications," *Progress in Electromagnetics Research C*, vol. 25, pp. 209-221, 2012.
- [35] J. S. Petko and D. H. Werner, "Miniature Reconfigurable Three-Dimensional Fractal Tree Antennas," *IEEE Transactions on Antennas and Propagation*, vol. 52, no. 8, pp. 1945-1956, August 2004.
- [36] A. Khidre, F. Yang and A. Z. Elsherbeni, "Circularly Polarized Beam-Scanning Microstrip Antenna Using a Reconfigurable Parasitic Patch of Tunable Electrical Size," *IEEE Transactions on Antennas and Propagation*, vol. 63, no. 7, pp. 2858-2866, July 2015.
- [37] D. Schaubert, F. Farrar, A. Sindoris and S. Hayes, "Microstrip antennas with frequency agility and polarization diversity," *IEEE Transactions on Antennas and Propagation*, vol. 29, no. 1, pp. 118-123, January 1981.
- [38] P. Bhartia and I. J. Bahl, "Frequency agile microstrip antennas," *Microwave Journal*, vol. 25, pp. 67-70, October 1982.
- [39] N. Fayyaz, S. Safavi-Naeini, E. Shin and N. Hodjat, "A novel electronically tunable rectangular patch antenna with one octave bandwidth," in *IEEE Canadian Conference on Electrical and Computer Engineering*, Waterloo, Ontario, Canada, 1998.
- [40] S. V. Hum and H. Y. Xiong, "Analysis and Design of a Differentially-Fed Frequency Agile Microstrip Patch Antenna," *IEEE Transactions on Antennas and Propagation*, vol. 58, no. 10, pp. 3122-3130, October 2010.
- [41] Y. Cao, S. W. Cheung and T. I. Yuk, "Frequency-reconfigurable multiple-input–multiple-output monopole antenna with wide-continuous tuning range," *IET Microwaves, Antennas & Propagation*, vol. 10, no. 12, pp. 1322-1331, 17 September 2016.
- [42] J. Costantine, C. C. G. and S. E. Barbin, "A new reconfigurable multi band patch antenna," in *SBMO/IEEE MTT-S International Microwave and Optoelectronics Conference*, Brazil, 2007.

- [43] M. Madi, K. Y. Kabalan and M. Al-Husseini, "Effect of Different Varactor Models on Antenna Tunability," in *International Conference on High Performance Computing & Simulation*, Genoa, Italy, 2017.
- [44] M. A. Madi, M. Al-Husseini, A. H. Ramadan, K. Y. Kabalan and A. El-Hajj, "A Reconfigurable Cedar-Shaped Microstrip Antenna for wireless Applications," *Progress in Electromagnetics Research*, vol. 25, pp. 209-221, 2012.
- [45] M. Mantash and T. A. Denidni, "Millimeter-wave Beam-Steering Antenna Array for 5G Applications," in *IEEE 28th Annual International Symposium on Personal, Indoor and Mobile Radio Communications*, Montreal, QC, Canada, 2017.
- [46] T. S. Rappaport, S. Sun, R. Mayzus, H. Zhao, Y. Azar, K. Wang, G. N. Wong, J. K. Schutz, M. Samimi and F. Gutierrez, "Millimeter Wave Mobile Communications for 5G Cellular: It Will Work!," *IEEE Access*, vol. 1, pp. 335-349, 2013.
- [47] Z. Zang, M. Su, H. Zhang, Y. Liu and K. Zhu, "A reconfigurable notch band UWB monopole antenna based on the split-ring resonators," in *International Symposium on Antennas and Propagation*, Phuket, Thailand, 2017.
- [48] S. F. Jilani and A. Alomainy, "Millimeter-wave conformal antenna array for 5G wireless applications," in *IEEE International Symposium on Antennas and Propagation & USNC/URSI National Radio Science Meeting*, San Diego, CA, USA, 2017.
- [49] A. V. Räsänen, J. Ala-Laurinaho, D. Chicherin, Z. Du, A. Generalov, A. Karttunen, D. Lioubtchenko, J. Mallat, A. Tamminen and T. Zvolensky, "Antennas for electronic beam steering and focusing at millimeter wavelengths," in *International Conference Electromagnetics in Advanced Applications*, Cape Town, South Africa, 2012.
- [50] E. Levine, G. Malamud, S. Shtrikman and D. Treves, "A study of microstrip array antennas with the feed network," *IEEE Transactions on Antennas and Propagation*, vol. 37, no. 4, pp. 426-434, April 1989.
- [51] M. T. Ali, T. A. Rahman, M. R. kamarudin and M. N. Md Tan, "A Planar Antenna Array with Separated Feed Line for Higher Gain and Sidelobe Level," *Progress in Electromagnetics Research C*, vol. 8, pp. 69-82, 2009.
- [52] S. H. Al-Charchafi and M. Frances, "Electronically tunable microstrip patch antennas," in *IEEE Antennas and Propagation Society International Symposium*, Atlanta, GA, USA, 1998.
- [53] S. H. Al-Charchafi and J. Kyriopoulos, "A varactor tuned microstrip patch antenna," in *Ninth International Conference on Antennas and Propagation*, Eindhoven,

Netherlands, 1995.

- [54] J. A. Zammit and A. Muscat, "Tunable microstrip antenna using switchable patches," in *Loughborough Antennas and Propagation Conference*, Loughborough, UK, 2008.
- [55] R. B. Waterhouse and N. V. Shuley, "Full characterisation of varactor-loaded, probe-fed, rectangular, microstrip patch antennas," *IEE Proceedings - Microwaves, Antennas and Propagation*, vol. 141, no. 5, pp. 367-373, October 1994.
- [56] S. Nikolau, R. Bairavasubramanian, C. Lugo, I. Carrasquilo, D. C. Thompson, G. E. Ponchak, J. Papapolymerou and M. M. Tentzeris, "Pattern and frequency reconfigurable annular slot antenna using PIN diodes," *IEEE Transactions on Antennas and Propagation*, vol. 54, no. 2, pp. 439-448, February 2006.
- [57] G. M. Rebeiz and J. B. Muldavin, "RF MEMS switches and switch circuits," *IEEE Microwave Magazine*, vol. 2, no. 4, pp. 59-71, December 2001.
- [58] M. A. Madi, M. Al-Husseini and K. Y. Kabalan, "Frequency Tunable Cedar-Shaped Antenna for WIFI and WIMAX," *Progress In Electromagnetics Research Letters*, vol. 72, pp. 135-143, 2018.
- [59] S. V. Shynu, G. Augustin, C. K. Aanandan, P. Mohanan and K. VAsudevan, "Development of a varactor-controlled dual-frequency reconfigurable microstrip antenna," *Microwave and Optical Technology Letters*, pp. 375-377, 2005.
- [60] N. Al Falahy and O. K. Y. Alani, "Design Considerations of Ultra Dense 5G Network in Millimeter Wave Band," in *2017 Ninth International Conference on Ubiquitous and Future Networks*, Milan, Italy, 2017.
- [61] "S.1151 : Sharing between the inter-satellite service involving geostationary satellites in the fixed-satellite service and the radionavigation service at 33 GHz," October 1995. [Online]. Available: <https://www.itu.int/rec/R-REC-S.1151/en>.
- [62] "Federal Spectrum Use Summary 30 MHz - 3000 GHz - National Telecommunications and Information Administration Office of Spectrum Management," June 21, 2010.
- [63] S. Methley, W. Webb, S. Walker and J. Parker, "5G Candidate Band Study - Study on the Suitability of Potential Candidate Frequency Bands above 6GHz for Future 5G Mobile Broadband Systems," ofcom, UK, 2015.